Manuscript Details

Manuscript number	BRB_2018_474_R1
Title	Investigating KYNA production and kynurenergic manipulation on acute mouse brain slice preparations
Article type	Research Paper

Abstract

Manipulation of kynurenic acid (KYNA) level through kynurenine aminotransferase-2 (KAT-2) inhibition with the aim of therapy in neuro-psychiatric diseses has been the subject of extensive recent research. Although mouse models are of particular importance, neither the basic mechanism of KYNA production and release nor the relevance of KAT-2 in the mouse brain has yet been clarified. Using acute mouse brain slice preparations, we investigated the basal and L-kynurenine (L-KYN) induced KYNA production and distribution between the extracellular and intracellular compartments. Furthermore, we evaluated the effect of specific KAT-2 inhibition with the irreversible inhibitor PF-04859989. To ascertain that the observed KYNA release is not a simple consequence of general cell degradation, we examined the structural and functional integrity of the brain tissue with biochemical, histological and electrophysiological tools. We did not find relevant change in the viability of the brain tissue after several hours incubation time. HPLC measurements proved that mouse brain slices intensively produce and liberate KYNA to the extracellular compartment, while only a small proportion retained in the tissue both in the basal and L-KYN supplemented state. Finally, specific KAT-2 inhibition significantly reduced the extracellular KYNA content. Taken together, these results provide important data about KYNA production and release, and in vitro evidence for the first time of the function of KAT-2 in the adult mouse brain. Our study extends investigations of KAT-2 manipulation to mice in a bid to fully understand the function; the final, future aim is to assign therapeutical kynurenergic manipulation strategies to humans.

Keywords	kynurenic acid, kynurenine aminotransferase-2 inhibition; acute slice viability; HPLC; immunohistochemistry; in vitro electrophysiology
Taxonomy	Neuropharmacology, Neurochemistry, Neurophysiology
Manuscript category	Neuropharmacological Mechanisms and Neurotherapeutics

Corresponding Author	Levente Gellert
Corresponding Author's Institution	Department of Physiology, Anatomy and Neuroscience, University of Szeged
Order of Authors	Judit Herédi, Edina Katalin Cseh, Anikó Berkó Magyariné, Gábor Veres, Dénes Zádori, Jozsef Toldi, Zsolt Kis, László Vécsei, Etsuro Ono, Levente Gellert

Suggested reviewers	Mihaly Hajos, Flavio Moroni, waldemar turski, Cheng Chang

Submission Files Included in this PDF

File Name [File Type]

CoverLetter_Ms_gl_2018_BRB_R1.docx [Cover Letter]

Answer to Reviewers.docx [Response to Reviewers]

BrainResearchBulletin_MS_R1.docx [Revised Manuscript with Changes Marked]

Highlights_R1.docx [Highlights]

Abstract_Ms_gl_2018_BRB_R1.docx [Abstract]

BrainResearchBulletin_MS_no highlight_R1.docx [Manuscript File]

Fig.1..tif [Figure]

Fig.2..tif [Figure]

Fig.3..tif [Figure]

Fig.4..tif [Figure]

Fig.5..tif [Figure]

Fig.6..tif [Figure]

KYNA 2-4-6_ng.tif [Figure]

GFAP 10x.jpg [Figure]

GFAP 40x.jpg [Figure]

GFAP_WB.tif [Figure]

Conflict of interest statement_Ms_gl_2018_BRB_R1.docx [Conflict of Interest]

Author declaration.pdf [Author Agreement]

BrainResearchBulletin_MS_Supplement_gl2018.doc [Supporting File]

To view all the submission files, including those not included in the PDF, click on the manuscript title on your EVISE Homepage, then click 'Download zip file'.

Research Data Related to this Submission

There are no linked research data sets for this submission. The following reason is given:
Data will be made available on request

Professor Beáta Sperlágh

Hungarian Academy of Sciences, Department of Pharmacology
H-1083 Budapest, Szigony utca 43.
Budapest, Hungary

Dear Professor Beáta Sperlágh,

please find attached our revised manuscript, entitled: **Investigating KYNA production and kynurenergic manipulation on acute mouse brain slice preparations**
First, we would like to thank you for the thorough review of the manuscript and for your helpful comments.
We have carefully read your letter and the Referees' evaluation sheet. We addressed their concerns, all of which helped shape the final, greatly improved manuscript. Changes in the manuscript have been indicated with red highlight. Furthermore, we performed additional experiments, and we created a new figure, a graphical explanation of our experimental protocol.

We think, that our study gives relevant addition to topic. As we posit in the MS, it is the first *in vitro* study with pharmacological KAT-2 manipulation in mice. Furthermore the acute slice viabilty evaluation makes the data more reliable, compared to former *in vitro* studies with rat. We think, we could extend the kynurenine and KAT-2 function modeling to the mouse, which was largely neglected in this relation.
We would be very grateful if our most recent data could be read in **Brain Research Bulletin**.
We hope you will consider our report worthy of acceptance.
We herewith make a clear statement that the work has not been published elsewhere, and it is not under review with another journal. All co-author agree with the submission of this form of the manuscript. We have read and have abided by the statement of ethical standards for manuscripts submitted to Brain Research Bulletin.

Sincerely your
Levente Gellért

Institute of Physiology,
University Medical Center of the Johannes Gutenberg University Mainz,
Duesbergweg 6, D-55128 Mainz,
Germany

Concerning Reviewer #1's comments:
We are extremely grateful for the Reviewer's comments, criticism and positive remarks; we addressed the Reviewer's concern on the optimal temperature for KAT-2 activity. Please find our answer and the change in the manuscript (red highlighted).

1. The Referee is correct, that KAT-2 has maximal activity *in vitro* around 50°C (Han et al., 2010). However, in this study it has been shown, that the activity of KAT-2 dramatically decreased after less than 50 min at 65°C, and was almost zero after 100 min. So, the incubation time at higher temperature is highly limited.
Indeed, 37°C would be closer to the physiological conditions, although for longer incubation it significantly decreases brain slice viability for many reasons (see, Buskila et al., 2014). Lower temperature can slow down these adverse processes and significantly prolong the time period during which the slices can be kept functional. Beyond tissue viability aspects, and *in vitro* electrophysiological routines we chose 30 °C for incubation basing on the paper of Banerjee et al. (2012), where this temperature was used as an optimal temperature for KAT-2. We completed the discussion with this issue (Page: 12, line: 349-356). Furthermore, we think, that the clear effect of the KAT-2 inhibitor indicates, that the KAT-2 enzyme was functional at 30 °C.

We hope that the Reviewer accepts our arguments. We would be grateful if the Reviewer could consider this manuscript acceptable for publication.

Best regards
Levente Gellért

Regarding Reviewer #2's comments:

We are very grateful for the Reviewer's comments, all of which helped shape the final, greatly improved manuscript. We addressed all of the Reviewer's concerns, and performed additional experiments. Furthermore, we created a new figure, a graphical explanation of our experimental protocol. Please find our answers in order of the comments. Please find the changes red-highlighted in the manuscript.

1. The Reviewer is correct. The original title highlights a result, which is an important point of the study, however it represents only partly the manuscript. Therefore we conceptualized a new title for the manuscript: Investigating KYNA production and kynurenergic manipulation on acute mouse brain slice preparations (Page: 1, line: 1-2)

Kynurenine evoked KYNA production means KYNA production upon L-kynurenine exposure. In the text we changed the former expression to “Kynurenine induced KYNA production” (Page: 13, line: 378).

2. a) We cut 6 coronal, 350 µm thick brain slices from the point Bregma -0,9 and halved every coronal slice for the SV and LV conditions, respectively, to compare the tissue quality. The same protocol was used in the case of studying KYNA production and kynurenergic manipulation in the SV condition. In every set of experiment, 6 halved slices were placed per chamber. We attached a figure about the protocol and presented it in the supplementary material (Page: 1, line: 22-26). Furthermore, we re-wrote this part of the manuscript in section 2.3 (Page: 4-5, line: 101-122).

b) Mice were taken arbitrarily from the home cage for every single experiment. For more detail, please see additional figure for experimental protocol (Supp. Fig. 1).

c) To guarantee the unity of the examined tissue in our study, we started to collect the 6 coronal slices from the most rostral part of the hippocampus (i.e. from Bregma -0,9mm to Bregma -3mm.). We always halved every slice for the two groups of a given experiment, so the same brain areas are involved in every set of experiment. See graphical explanation of tissue processing (Supp. Fig. 1).

d) The Reviewer is correct again. Incubation of rat cortical slices under non-oxygenated conditions caused marked suppression of KYNA synthesis (Turski et al., 1989). During incubation we maintained constant temperature under atmospheric pressure, conditions under which continuous carbogenation (continuous bubbling through thin plastic tube) keeps the solubility and availability of oxygen constant, according to Henry’s law. Before placing the slices into the small chamber we pre-carbogenated the ACSF to stabilize solved oxygen level and pH. After incubation we did not notice any pH declination, which also indicates an unchanged solved oxygen level.

e) We created an additional figure about the protocol to the supplement material (see. Supp. Fig. 1).

3. The Reviewer is absolute right that normalization of measured data to protein content is a widely applied method. However, according to our previous experiences, in case of brain samples, this normalization did not really decrease the deviation of data compared to when the results were normalized to wet weights. The wet weight is approximately ten times larger than protein content in case of brain samples. So we chose normalization to wet weight which is a widely applied approach in neuroscience research as well (Rushaidhi et al., 2012; Walczak et al., 2014).

4. The Reviewer is correct that the justification of the 4 hours long incubation was not clarified in the text. Our aim was to use the possible longest incubation time without losing tissue functionality. We performed additional experiments and examined the L-KYN induced

KYNA production after 2 hours long incubation (see the attached figure, where control is 4h incubation without L-KYN). We found, that there is no sufficient KYNA increase in the L-KYN treated group on which the inhibition of KYNA synthesis could reliably be studied. We completed the text in the Discussion section with this additional result (Page: 11-12, line: 328-332).

Figure 1.

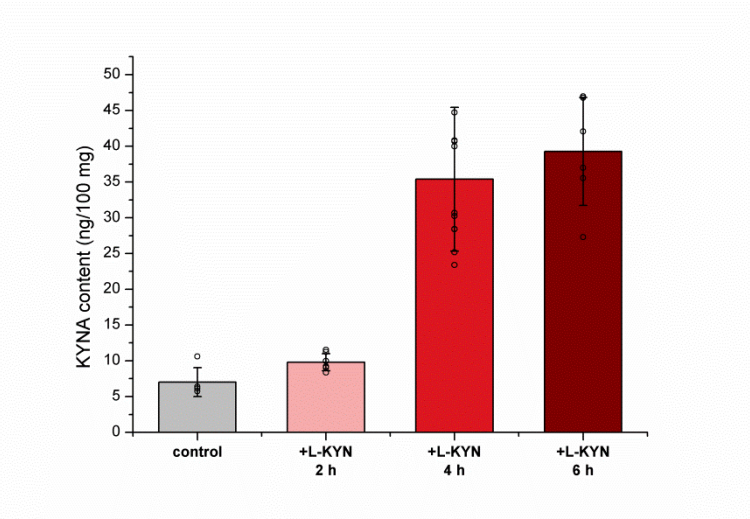

Extracellular KYNA content after various incubation time. Control: 4h incubation without L-KYN supplement. 2-4-6h: incubation along L-KYN supplementation. 4h incubation results in a relevant increase of KYNA production, compared to 2h incubation.

It is also true, that glucose deprivation can cause marked suppression of KYNA synthesis in acute brain slices (Turski et al., 1989). The glucose content indeed decreased significantly in our system after 4 h incubation. However, the standard ACSF solution contains a significantly higher concentration of glucose (10 mM) than that in the cerebrospinal fluid (0.47 – 4.4 mM) *in vivo*. A previous study showed that decreasing glucose content of the ACSF from 10 mM to 5 mM resulted in no disruption in synaptic function and metabolic capacity of brain tissue (Sadgrove et al., 2007). So we think that the observed decrease of glucose does not harm the tissue functionality; glucose is available for the slices in the ACSF in at a sufficient level (~ 8 mM).

Furthermore, the increased LDH level indicate cell membrane dysfunction, however the considerably higher LDH content of the supernatant ACSF after membrane permeabilization with Triton-X-100 indicates that after 4h incubation membrane integrity of the nervous tissue is largely preserved. Electrophysiological data support this assumption as well. Basal glutamatergic synaptic properties were equally functional in the compared groups, so the functional integrity of this vulnerable region was largely preserved.

5. Our aim was to test whether the general tissue integrity is preserved after 4h incubation in our system to avoid making false conclusions from a massively injured tissue. To this end,

we performed the electrophysiological, biochemical and histological studies mostly targeting neuronal function.

Indeed, the Reviewer is right; mechanical (vibratome slicing) and osmotic stress, temporary anoxia and exposure to cytosolic and blood born components may initiate altered glial function in acute brain slices (Takano et al., 2014).

Morphological changes of astrocytes (e.g. retraction of fine processes) are signs of early-stage astrogliosis (Takano et al., 2014). In additional experiments we made comparisons of astrocyte morphology and GFAP expression under LV and SV conditions after 4h incubation. In the hippocampus we did not detect any visible difference in the morphology of glia cells (see the attached image of LV (left panel) and SV (right panel) group). Furthermore, we found only slight, not significant elevation of GFAP protein level after 4h SV incubation, compared to LV group (see figure 2). We agree, that this alteration may be the sign of accommodating glial function, however, we think, that, this is not equal to glial malfunction. Furthermore level of KAT-2 protein, which is mostly expressed by the astrocyte, was not altered (see supplementary material in the manuscript). This also supports a normal glial KAT-2 function throughout the 4h incubation.

Figure 2.

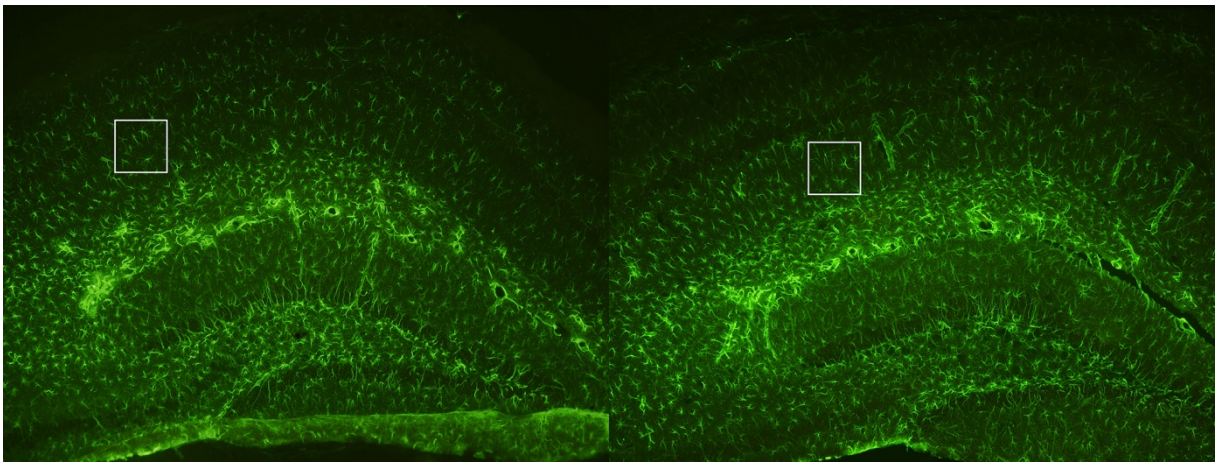

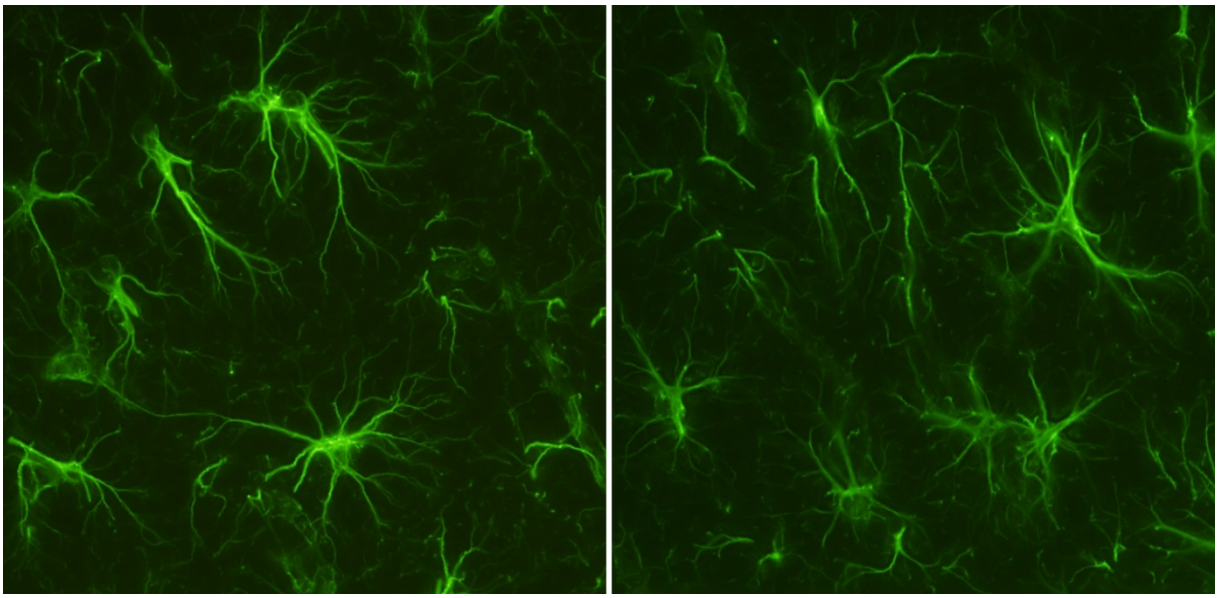

Fluorescent photomicrograph (100x magnification) of hippocampal slices incubated either under LV (left panel) or SV condition for 4h. High magnification of insets in the same order. No visible difference of cell shape and fine process morphology between the two groups after 4h incubation.

Figure 3.

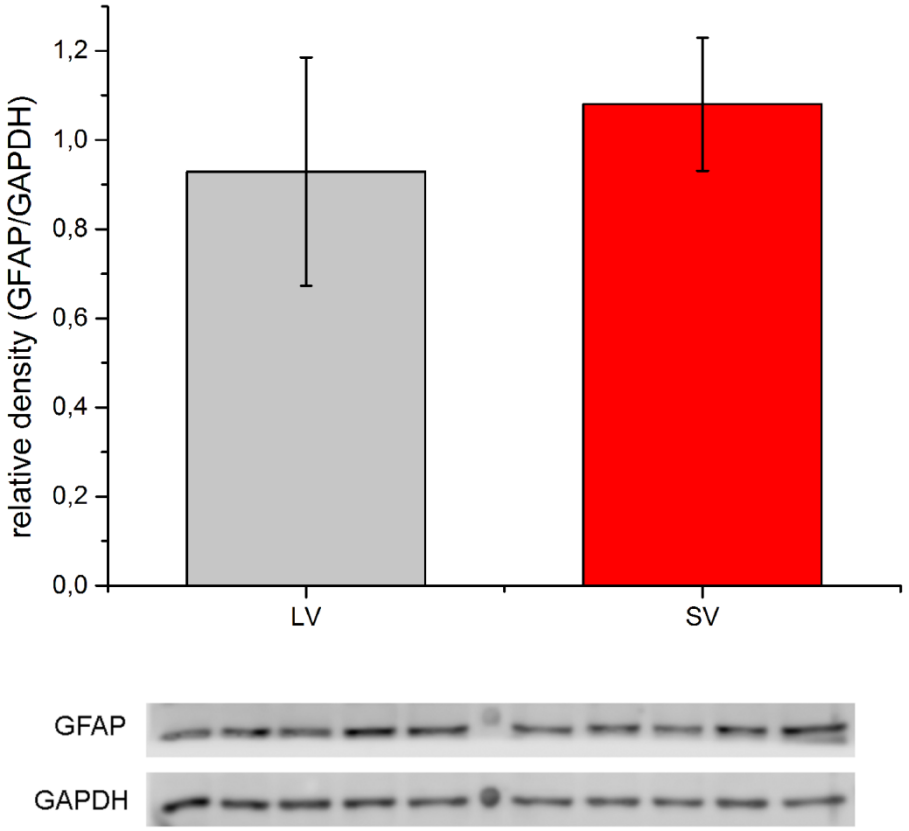

Relative GFAP expression level of LV and SV samples after 4h incubation. Modest, but not significant elevation of GFAP protein level in the SV group.

6. The Reviewer is right, that the goal of the study should be formulated in one or some focused points. However, we tried to fill gaps of three diverse tracks in Kynurenine research. 1. to our best knowledge, to date there is no data about the effect of pharmacological KAT-2 manipulation in mice, 2., yet, the intra/extracellular distribution of kynurenic acid , and the effect of L-Kynurenine supplementation are not clarified, and 3., the acute slice viabilty evaluation makes the data more reliable, compared to former *in vitro* studies with rat. Indeed, a focused scientific question we did not formulate, instead we gave clear explanation in the introduction session, why we need these experiments to extend the kynurenine and KAT-2 function modeling to the mouse, which was largely neglected in this relation.

We hope that the Reviewer accepts our arguments. We would be grateful if the Reviewer could consider this manuscript acceptable for publication.

Best regards

Levente Gellért

Banerjee et. al, J Pharmacol Exp Ther. 2012 May;341(2):500-9. doi: 10.1124/jpet.111.189860.

Buskila et. al, Sci Rep. 2014 Jun 16;4:5309. doi: 10.1038/srep05309.

Han et. al, BMC Biochem. 2010 May 19;11:19. doi: 10.1186/1471-2091-11-19.

Rushaidhi et. al, Neuroscience. 2012 May 3;209:21-31. doi: 10.1016/j.neuroscience.2012.02.021.

Sadgrove et. al, Brain Res. 2007 Aug 24;1165:30-9.

Takano et. al, Glia. 2014 Jan;62(1):78-95. doi: 10.1002/glia.22588.

Turski et. al, J Neurochem. 1989 May;52(5):1629-36.

Walczak et. al, Pharmacol Rep. 2014 Feb;66(1):130-6. doi: 10.1016/j.pharep.2013.06.007.

Investigating KYNA production and kynurenergic manipulation on acute mouse brain slice preparations

Judit Herédi[1], Edina Katalin Cseh[2], Anikó Magyariné Berkó[1], Gábor Veres[2], Dénes Zádori[2], József Toldi[1], Zsolt Kis[1],László Vécsei[2,3],Etsuro Ono[4];Levente Gellért[1,*]

[1]Department of Physiology, Anatomy and Neuroscience, Faculty of Science and Informatics, University of Szeged, Közép Fasor 52., Szeged 6726, Hungary.

[2]Department of Neurology, Faculty of Medicine, University of Szeged, Semmelweis st.6, Szeged 6725 Hungary

[3]MTA-SZTE Neuroscience Research Group, University of Szeged, Semmelweis st. 6, Szeged 6725, Hungary.

[4]Department of Biomedicine, Graduate School of Medical Sciences, Kyushu University Fukuoka, Japan; Center of Biomedical Research, Research Center for Human Disease Modeling, Graduate School of Medical Sciences, Kyushu University Fukuoka, Japan.

[*]Correspondence: Levente Gellért, Department of Physiology, Anatomy and Neuroscience, University of Szeged, Közép fasor 52, Szeged, H-6726, Hungary
e-mail: gellert.levente1@gmail.com

Keywords: kynurenic acid, kynurenine aminotransferase-2 inhibition; acute slice viability; HPLC; immunohistochemistry; in vitro electrophysiology

1 Introduction

Tryptophan (TRP) is catabolized mostly through the kynurenine pathway (KP) in the mammalian brain (Gal and Sherman 1980). Kynurenic acid (KYNA) is one of the neuroactive products of this metabolic route. KYNA is synthesized with the irreversible transamination of L-kynurenine (L-KYN), a reaction catalyzed by kynurenine aminotransferases (KATs) (Han et al., 2010a). KYNA exerts multiple effects on ligand-gated ion channels (Gal and Sherman, 1980, Birch et al., 1988, Prescott et al., 2006, Albuquerque and Schwarcz, 2013) and on the G-protein-coupled receptor 35 in the brain (Berlinguer-Palmini et al., 2013, Alkondon et al., 2015). Through these actions, KYNA can modulate neurotransmission systems (Zmarowski et al., 2009, Alexander et al., 2012, Banerjee et al., 2012a, Olsson et al., 2012). Indeed, the role of KYNA in neurophysiological and neuropathological processes has been the subject of extensive contemporary studies. The causal role of diversion of the KP has been proposed in several neurodegenerative and neuropsychiatric disorders (e.g. Alzheimer's disease, Parkinson's disease, Huntington's disease, cerebral ischemia, depression, and schizophrenia) (Vecsei et al., 2013). Thus, kynurenergic manipulation with the aim of therapy has also been proposed (Amaral et al., 2013).

To date, cross-species differences of the relevance and regulation of brain KP function and KYNA production are not fully clarified. The majority of the experimental data concerns the rat kynurenine system, however, mouse models are of particular importance as well (Rosenthal and Brown, 2007).

Yet, there is neither detailed study about the mechanism and regulation of KYNA release from cells in the mouse brain parenchyma, nor information about the function of relevant KAT enzymes of the KP. For instance, the importance of kynurenine aminotransferase-2 (KAT-2) in the rat and human brain is unequivocal, the relevance of KAT-2 in the mouse brain is, however, controversial (Han et al., 2010a).

For describing the kynurenine system in model animals and investigating the effect of kynurenergic manipulation, *in vitro* models are essential and complement *in vivo* studies. To this end, acute brain slice preparations provide many advantages over *in vivo* experiments (Cho et al., 2007, Lein et al., 2011). Previously, KYNA production and release to the extracellular compartment upon L-KYN exposure was described in cortical (Turski et al., 1989, Hodgkins et al., 1999) and in hippocampal rat brain slices (Scharfman et al., 1999, Alkondon et al., 2011). However, there is no data about KYNA production of acute mouse brain slice preparations. Furthermore, these studies did not concern the acute slice viability, a factor, which can strongly influence the KYNA production and release.

55 The present study was designed to estimate the KYNA production and release of acute mouse
56 brain slices and to assess the effect of the specific KAT-2 inhibitor PF-04859989 on KYNA
57 production *in vitro.*
58 Basing on literature data we presumed that the concentration of KYNA released into the
59 extracellular space falls into the picomolar or low nanomolar range (Schwieler et al., 2006).
60 To ensure a measurable concentration of KYNA for HPLC assessments we incubated our
61 slices in a low bulk volume of artificial cerebrospinal fluid (aCSF) (that is approx. 6 ml of
62 aCSF/100mg wet weight brain tissue) under continuous carbogenation, but without perfusion.
63 In previous studies KYNA increase and release could be measured 2-4hours after L-KYN
64 administration in rat (Turski et al., 1989, Swartz et al., 1990). Results of our pilot experiments
65 are in line with that finding (unpublished data). Therefore, we decided to incubate brain slices
66 for 4-6 hours. Incubation of acute slices inherently initiates progressive damage in the tissue
67 (Fukuda et al., 1995). It is therefore possible that metabolic properties and integrity of cells
68 involved in KYNA production and release might alter during several hours of incubation. In
69 order to characterize the after-incubation viability of the brain tissue we performed
70 histological observations, biochemical and electrophysiological characterization of the slices.
71 To investigate the extra/intracellular distribution of basal KYNA, we compared the KYNA
72 content in the tissue with that liberated into the extracellular space. Then, we wanted to know
73 if we could induce *de novo* KYNA production with the administration of the KYNA precursor
74 L-KYN. Finally, we investigated the effect of the KAT-2 inhibitor on the L-KYN-induced
75 KYNA release.
76 Investigating tissue viability, we found a slight alteration in some of the observed tissue
77 viability measures. However, the slices showed no anatomical or functional abnormalities, so
78 tissue integrity was preserved.
79 Regarding KYNA production, we found that in the course of 4hours incubation slices readily
80 release both basal and *de novo* produced KYNA into the supernatant aCSF, whereas only a
81 negligible fraction of total KYNA is retained in the tissue. The KAT-2 inhibitor, however,
82 conspicuously decreased KYNA release.
83

2 Experimental Procedures

2.1 Animals

8-12 weeks old male *C57Bl/6* mice obtained from The National Institute of Oncology (Budapest, Hungary) were used (n=30) for the experiments. Animals were kept under controlled laboratory conditions and had free access to food and water. All experiments were in compliance with the guidelines of the European Communities Council Directives (2010/63/EU) and the Hungarian Act for the Protection of Animals in Research (XXVIII.tv. 32.§).

2.2 Acute slice preparation

Animals were anesthetized with isoflurane (3%) followed by decapitation (NEMI Guillotine; Braintree Scientific, Inc.). The brain was rapidly removed and submerged in ice-cold aCSF (pH 7.4) composed of (in mM): 234 sucrose, 3.5 KCl, 1 NaH_2PO_4, 24 $NaHCO_3$, 1 $CaCl_2$, 3 $MgSO_4$ and 10 D-glucose (Sigma Aldrich) and oxygenated with 95% O_2 and 5% CO_2. 350 µm thick sections were obtained with a vibratome (Leica VT1200S, Germany); the two hemispheres were dissected and transferred to a holding chamber. Slices were allowed to recover for 30 min in aCSF (pH 7.4) containing (in mM): 130 NaCl, 3.5 KCl, 1 NaH_2PO_4, 24 $NaHCO_3$, 1.5 $CaCl_2$, 3 $MgSO_4$ and 10 D-glucose

2.3 Small volume incubation of brain slices

After 30 min recovering, one hemisphere of the 6 coronal slices were transferred to the incubation chambers containing a low bulk volume of aCSF (appr. 6ml of aCSF/6 half coronal slice), placed on a closed-loop temperature controller pad (TMP-5b, Supertech Instruments UK Ltd.) at 30 °C to reach optimal temperature for KAT function (Banerjee et al., 2012b) **(SV condition hereafter)**. The aCSF was continuously bubbled with 95% O_2 and 5% CO_2 but was not circulated during the incubation.

For comparison of tissue viability of slices incubated in SV condition or in standard condition, we performed the same battery of experiments on the corresponding 6 half coronal slices kept under standard conditions (high bulk volume of aCSF; ≈200ml/6 half coronal slice) at 20 °C **(LV condition hereafter)**. Through this LV slice incubation routine we could perform stable field excitatory postsynaptic potentials (fEPSP) recordings after 8h incubation, therefore, this condition was used as an adequate control for assessing tissue viability under SV condition.

115 After evaluating tissue viability, we studied KYNA production and kynurenergic
116 manipulation in the SV condition. 10 µM L-KYN (Sigma Aldrich) and 5 µM KAT-2 inhibitor
117 PF-04859989 were dissolved in aCSF. The scheme of the protocol used in this study is
118 illustrated in **Supp. Fig. 1.**
119 At the end of the incubations, the supernatants were collected and stored at -80 °C for further
120 biochemical analysis. One portion of the slices were placed in 4% paraformaldehyde (PFA)
121 and fixed overnight for histological studies, whereas the remaining slices were immediately
122 frozen in liquid nitrogen and stored at -80 °C for Western blotting (see in the supplement).

123 **2.4 Electrophysiology**

124 After 4h incubation in the LV or SV condition, the slices were transferred to an interface
125 recording chamber and superfused with aCSF containing (in mM): 130 NaCl, 3.5 KCl, 1
126 $NaH2PO_4$, 24 $NaHCO_3$, 3 $CaCl_2$, 1.5 $MgSO_4$ and 10 D-glucose. The temperature (32 °C) and
127 flow rate (2 ml/min) of the aCSF were continuously controlled. Baseline synaptic function of
128 the tissue was tested with input-output (I/O) curve recordings on the CA3-CA1 cell synapses
129 in the hippocampus. Schaffer collaterals were stimulated at 0,05 Hz using a concentric bipolar
130 stainless steel electrode (Neuronelektrod Ltd, Hungary). fEPSPs were recorded from the
131 stratum radiatum of CA1 region with 1,5–3 mOhm resistance glass microelectrodes.
132 Potentials were amplified and filtered with WPI AMP-04 amplifier and digitalized with Axon
133 Digidata 1320A. Recordings were monitored and saved with Axoscope 10.0 (Molecular
134 Devices Corporation, USA). Data were analyzed with Clampfit 10.6 (Molecular Devices,
135 USA) and OriginPro 8.6 (OriginLab Corporation, USA) softwares. In the course of I/O curve
136 recordings to define the minimal stimulus we decreased the stimulus intensity until minimal
137 but unequivocal fEPSP was evoked. The stimulus was then increased in 5 µA increments. We
138 collected five responses and averaged at each increment. We continued to increase the
139 stimulus intensity until fEPSP response had saturated. fEPSP slope values were normalized
140 and averaged across all slices in each group and plotted as a function of normalized stimulus
141 intensity to construct I/O curves.

142 **2.5 Histology**

143 Fixed brain slices were cryoprotected with sucrose solution and 30 µm thick sections were cut
144 with a freezing microtome (Reichert-Jung 1206).
145 *Immunohistochemistry:* Free-floating sections were washed in PBT, incubated in 1% NDS
146 and exposed to the primary antibody (mouse anti-NeuN, 1:4000, Millipore) overnight at 4 °C.

147 Next day, they were incubated in the appropriate secondary antibody (1:500; Jackson
148 ImmunoResearch) at room temperature. Primary and secondary antibody were diluted in 0.1
149 M PBT containing 1% NDS. Negative control was prepared from sections incubated without
150 the primary antibody. The sections were coverslipped with antifade mounting medium
151 (ProLong® Gold, Life Technologies).
152 *Cresyl violet staining:* We performed cresyl violet staining for morphological observations
153 after different incubation conditions and time. Sections were rehydrated with descending
154 grades of alcohol and stained with cresyl violet staining solution for 5 min. After staining,
155 samples were passed through ascending alcohol solutions and immersed in xylene for 5 min.
156 Sections were coverslipped with Entallan®.
157 All photomicrographs were obtained with an Olympus BX51 microscope fitted with a DP70
158 digital imaging system.

159 **2.6 Lactate dehydrogenase (LDH) assay**

160 For evaluating tissue viability we performed LDH activity assay on supernatant samples
161 collected after 30 min, 4h and 6 h incubation time. As positive control for LDH release we
162 permeabilized the cell membrane with Triton X-100™ (1%). LDH activity was measured at
163 340 nm and 37 ˚C using an LDH activity assay kit (Diagnosticum Ltd, Hungary, 46461) on a
164 BioLis 24i Premium system (Siemens). LDH activity was expressed as U/l/100 mg tissue.

165 **2.7 Hexokinase (HK) assay**

166 Glucose content was measured by HK activity assay on supernatant samples collected after 30
167 min, 4h and 6h incubation time. HK activity was measured at 340 nm and 37 ˚C using a two-
168 step Glu HK activity assay kit (Diagnosticum Ltd, Hungary, 47361) on a BioLis 24i Premium
169 system (Siemens).

170 **2.8 High performance liquid chromatography (HPLC)**

171 The brain slices were weighed and then homogenized for 30s in 250 ml ice-cold solution,
172 containing trifluoroacetic acid (0.1% v/v) and 2 µM 3-nitro-L-tyrosine (3-NLT, as internal
173 standard). The homogenate was centrifuged at 12000 RPM for 10 min at 4°C. The
174 supernatants were stored at -80°C until further analysis. Similar procedure was applied for the
175 aCSF samples, briefly, 250 µL aCSF was treated with 50 µl of above-mentioned solution, and
176 then centrifuged under the same circumstances as the brain tissues. The resulting supernatants
177 were measured with an Agilent 1100 HPLC system (Agilent Technologies, Santa Clara, CA,
178 USA) combined with a fluorescence (FLD) and a UV detector. For the determination of

179 KYNA, the excitation and emission wavelengths of FLD were set at 344 nm and 398 nm,
180 whereas the UV detector was set at 365 nm for the determination of 3-NLT. Chromatographic
181 separations were performed on an a Kinetex C18 column, 150 x 4.6 mm I.D., 5 µm particle
182 size (Phenomenex Inc., Torrance, CA, USA) preceded by Security Guard pre-column C18, 4
183 x 3.0 mmI.D., 5 µm particle size (Phenomenex Inc., Torrance, CA, USA) with a mobile phase
184 composition of 0.2 M zinc acetate/ACN = 95/5 v/v%, in which pH was adjusted at 6.2 with
185 acetic acid, applying isocratic elution. The flow rate was 1.2 ml/min and the injection volume
186 was 50 µL. As for the method validation, following parameters are reported, briefly,
187 regarding KYNA in tissue and aCSF. The LOD and LOQ in tissue and aCSF samples were 1
188 and 3.75 nM, respectively. With regard to precision, the relative standard deviation was ≤
189 2.2%. The recoveries in tissue and aCSF samples ranged from 103% to 108% and 81% to
190 91%, respectively.

191 **2.9 Data analysis and Statistics**

192 KYNA content was calculated from the concentration values measured by HPLC and data
193 were normalized to the tissue weight. In the case of the aCSF, values represented KYNA
194 content released by 100 mg tissue. LDH release and glucose consumption data were similarly
195 normalized to 100 mg tissue.
196 All statistical computations were carried out with the IBM SPSS Statistics software (version
197 20.). Homogeneity of variance across groups was tested with the Levene's Test of Equality of
198 Error Variances. Distribution of the data was tested with the-Shapiro-Wilk test of normality.
199 Statistical significance was calculated with the GLM univariate model. If assumption of
200 variance homogeneity was violated, Kruskal-Wallis Test was used. For repeated measures of
201 the I/O curve recordings, General Linear Model Repeated Measures method was applied.
202

3 Results

3.1 Glucose consumption

To our best knowledge, there is no literature data about the minimal bulk volume of aCSF in which acute mouse brain slices can function quasi normally for hours. Therefore, first, we asked if the glucose availability in the aCSF under SV condition exceeds the nutrition demand of the slices.

Glucose consumption measurement proved that glucose availability gradually decreased during the incubation. Glucose concentration was already dropped after 30 min, however, the decrease was not statistically significant (F=4,281; p=0,072; Partial Eta Squared: 0,349). 4h incubation, however, resulted in a significant decrease of aCSF glucose content (F=20,304; p=0,002; Partial Eta Squared: 0,717) compared to original level (**Fig. 1).** It was further declined during the 6h incubation time (data not depicted).

3.2 Viability of acute brain slices – LDH release

A characteristic sign of the perturbation of normal cellular function is the loss of cell membrane integrity and the concomitant increase of membrane permeability (Cho et al., 2007). Therefore, alteration in LDH release to the extracellular space is a sensitive measure of cell viability. Under SV condition LDH release was continuously increasing in the aCSF during 30 min (Z= 16,910; p=0,959), 4h (Z= 16,910; p=0,030) and also 6 h incubation (data not depicted), compared to the initial state. However, Triton X-100 treatment resulted in a ≈14 fold increase of LDH in the aCSF after 4h incubation (Z= 16,910; p=0,001) **(Fig. 2)**. This indicates that the cell membrane integrity is largely preserved in the course of 4h incubation. The observed KYNA release is not the simple consequence of disrupted membrane integrity (see below).

3.3 Histological observations

For the histological examination of tissue state we performed NeuN immunolabelling and cresyl violet staining. There was no visible tissue damage in the vulnerable CA1 subregion of the dorsal hippocampus. CA1 pyramidal cell shape and size appeared normal after 4h incubation **(Fig. 3)**. However, the structural integrity of pyramidal cells in CA1 was not completely preserved after 6h incubation. Compared to the control group, shrunken and deformed pyramidal cells emerged (visual observation).

235 **3.4 Synaptic properties of acute brain slices - I/O curves**

236 Basal glutamatergic synaptic properties were tested by means of fEPSP recording, expressed
237 against gradually increased stimulating intensity in certain groups. There was no significant
238 difference between slices recorded immediately after post-slicing recovery period (30 min.),
239 or incubated under LV condition for 4hours and under SV conditions, respectively (F=0.793;
240 p=0,465; Partial Eta Squared: 0,064). This result indicates that, the baseline synaptic function
241 of the brain tissue was preserved after 4h SV incubation **(Fig. 4)**.

242 Considering the decreased glucose availability and increased LDH release, furthermore the
243 visually observed tissue damage after 6 h, the 4h long incubation duration was considered to
244 be the most suitable for KYNA measurement.

245 **3.5 KYNA production in mouse brain slices**

246 To examine whether mouse brain slices liberate endogenous and *de novo* produced KYNA
247 upon L-kynurenine administration during 4h long incubation period we performed HPLC
248 measurements from brain tissue homogenate and from incubating aCSF.
249 Without L-KYN administration 7.01±2.03ng basal KYNA content could be measured from
250 the aCSF and 0.22±0.07ng from the brain tissue homogenate. In contrast, as a result of 10 µM
251 L-KYN administration we found a 6.3 fold increase in the aCSF (44.56 ±6,99ng) (Z=6,818;
252 p=0,009) and a 3.8 fold increase in the tissue (0.85±0.21ng) KYNA content **(Fig. 5)**. No
253 considerable KYNA elevation could be observed in the course of 6h incubation compared to
254 the 4h incubation (data not depicted).
255 In conclusion, ≈97% of the total KYNA content was released to the extracellular
256 compartment (aCSF), whereas only ≈3% remained in the tissue under both conditions **(Supp.**
257 **Fig. 2)**

258 **3.6 Effect of KAT-2 inhibitor PF-04859989 on *de novo* KYNA release**

259 In the next series of experiments we incubated acute slices in the presence of 10 µM L-KYN,
260 with or without PF-04859989 in a concentration of 5µM. KYNA content of the aCSF was
261 measured after 4h incubation. Similar to former results high KYNA content could be
262 measured in the L-KYN group (55.19±6.45ng). Addition of the inhibitor resulted in a
263 significant decrease of the released KYNA in the aCSF by almost 40% (34.5±6.93ng;
264 F=23,868; p=0,001; Partial Eta Squared: 0,749) **(Fig. 6).**

4 Discussion

The implication of kynurenine metabolites in several brain disorders (e.g. schizophrenia, Alzheimer's disease, depression, migraine) shifted much attention to the manipulation of the KP in recent years (Dounay et al., 2015). The KP of tryptophan catabolism is present in many mammalian species (Moroni et al., 1988). Concomitantly, the neuromodulatory metabolites of this route are produced and function, making model animals suitable for extrapolating the effects of kynurenergic manipulation in humans. However, there are prominent differences among mammalian species regarding the kynurenine system (Moroni et al., 1988, Fujigaki et al., 1998), complicating further the understanding of the physiological and pathological role of the KP.

The physiological concentration of KYNA is different in model animals and in humans. The lowest basal KYNA level is found in the mouse brain, whereas it is the highest in the human neocortex (Moroni et al., 1988). The KYNA synthesizing enzyme isoforms have also a different role in different species. In the human and rat brain KAT-2 plays the major role in KYNA production, whereas in mice kynurenine aminotransferase-4 (KAT-4) was supposed to be the main KYNA synthesizing enzyme (Alkondon et al., 2004, Guidetti et al., 2007). However, KAT-2 null mutation resulted in the decrease of extracellular KYNA level in transgenic mice (Potter et al., 2010). Therefore, comparative characterization of the kynurenine catabolism in different model species is essential before assigning therapeutical kynurenergic manipulation strategies in humans.

Investigating the KP *in vitro* is of particular importance. In contrast to *in vivo* assays, acute brain slice preparations provide the possibility to exclude the perturbation effect of the peripheral KP function, while replicating or even changing many aspects of the *in vivo* context. A large panel of pharmacological interventions can be efficiently evaluated; furthermore, endogenous factors influencing brain KYNA production might also be easily clarified.

4.1 The after-incubation state of mouse brain slice preparations

One of the major limitations of acute brain slice models is the viability of nervous tissue, which endures on average for ≈ 6-8 hours (Buskila et al., 2014). However, there are specific brain areas (e.g. dorsal hippocampus) and cell populations where this window is even narrower (≈4hours) (Fukuda et al., 1995). To ascertain that KYNA release is not an uncontrolled function of a deteriorated brain tissue, we examined the after-incubation

297 viability. After 4h and 6h incubations in the SV aCSF, respectively, we observed slight
298 alterations in tissue integrity and function.
299 The change of cell membrane integrity was evaluated by measuring the cytosolic LDH
300 released into the aCSF. LDH could be measured and was continuously increasing during the
301 incubation time, a phenomenon that verifies the limited and relatively narrow working
302 window with acute brain slices. The considerably higher LDH content of the supernatant
303 aCSF after membrane permeabilization indicates that after 4h incubation membrane integrity
304 of the nervous tissue is largely preserved.
305 Changes in glucose consumption and glucose availability we estimated with a glucose
306 hexokinase assay. We found that the available glucose was gradually decreased in the course
307 of 4h and 6h incubation (not depicted). Although, continuous aCSF LDH level increase
308 suggests a gradual loss of membrane integrity, decrease of glucose availability in the course
309 of 4h and 6h incubation is possible only if, the nervous tissue actively metabolizes glucose. In
310 the nervous tissue both astrocytic and neuronal glucose up-take is possible through facilitative
311 membrane glucose transporters (Chuquet et al., 2010, Lundgaard et al., 2015). A shift toward
312 one of these mechanisms we did not estimate, however we may conclude a generally
313 preserved glucose up-take, consumption-machinery and functioning brain tissue.
314 Although the selective vulnerability of the CA1 region of the hippocampus to a variety of
315 insults (e.g. excitotoxicity, cerebral ischemia) has been reported (Davolio and Greenamyre,
316 1995, Kovalenko et al., 2006) we observed no visible tissue damage in this brain area.
317 Furthermore, Schaffer-collateral CA1 pyramidal cell synapses were equally functional in the
318 compared groups. There was no significant difference between slices recorded immediately
319 after post-slicing recovery period (30 min.), or incubated under LV condition for 4hours and
320 under SV conditions, respectively. This indicates that functional integrity of vulnerable region
321 was largely preserved during a 4h SV incubation.

322 **4.2 Basal and *de novo* KYNA production in mouse brain slices**

323 Our first and basic question was, whether KYNA production can be measured and elevated in
324 mouse brain slice preparations. To increase KYNA production L-KYN concentration (10 μM)
325 was chosen on the basis of previous studies on slice preparations (Urbanska et al., 2000,
326 Okuno et al., 2011). Similar to rat brain slices (Alkondon et al., 2011), mouse brain slices
327 could produce KYNA upon L-KYN exposure and liberate newly formed KYNA to the
328 extracellular space after 4h incubation **(See Fig. 5.)**. In trial experiments we measured KYNA
329 production after 2h incubation, but there was no sufficient KYNA increase in the L-KYN

330 treated group on which the inhibition of KYNA synthesis could reliably be studied (not
331 depicted). Therefore, 4 h long incubation was necessary to examine KYNA production and
332 the effect of KAT-2 inhibition.
333 It is important to note that, extending the extracellular space of the acute slices with the
334 incubating aCSF (approx. 100 mg wet weight brain tissue/6ml aCSF) results in a considerably
335 smaller intracellular/extracellular volume ratio than found in the intact mouse brain (approx.
336 500mg wet weight brain tissue/0,04ml CSF (Artru, 1993). That difference means a steep
337 concentration gradient and driving force toward the aCSF for any released molecules. After
338 4h incubation the amount of the released KYNA was more than 30 times higher than that
339 retained in the tissue **(See Supp. Fig. 2.)**. This release mechanism of KYNA is still unknown
340 and should also be investigated in future work. Nevertheless, a high local KYNA
341 concentration might be reached upon L-KYN treatment in the close apposition of the KYNA
342 release sites.
343 It is important to note that our results regarding KYNA production may not reflect completely
344 the *in vivo* mechanisms. The brain-to-blood elimination of brain KYNA through probenecid-
345 sensitive organic acid transport is continuous *in vivo* (Miller et al., 1992), however, the ratio
346 of elimination in the mice is not described. Furthermore, the composition of aCSF differs in
347 several aspects from the *in vivo* physiological extracellular milieu. For instance, there are no
348 amino acids in the aCSF (e.g. aspartate, tryptophan), which can negatively impact the activity
349 of the KAT isoenzymes (Han et al., 2010b). The applied incubation temperature was lower
350 than physiological, but higher temperature curtails the lifespan of acute slices as a
351 consequence of bacterial growth and cellular metabolism (Buskila et al., 2014). Lower
352 temperature slows down these adverse processes and prolong the time period during which
353 the slices can be kept functional. Beyond tissue viability aspects, and *in vitro*
354 electrophysiological routines we chose 30 °C for incubation basing on the paper of Banerjee
355 et al. (2012), where this temperature was used as an optimal temperature for KAT-2 (Banerjee
356 et al., 2012). These differences may lead to altered KAT activity and to a modified
357 production of KYNA. However, we did not find altered KAT-2 expression level of the
358 samples incubated under SV condition (F = 0.000; p =0.989; Partial Eta Squared: 0.000),
359 therefore a quasi normally KYNA production can be suggested **(Supp. Fig. 3).**

360 The ≈6.3fold elevation in aCSF KYNA content by this small amount of tissue after L-KYN
361 addition indicates a high KAT capacity. Previously it has been shown on purified KAT
362 preparation from rat liver that KATs have high capacity and Km value (~1 mM) for L-KYN

363 (Bender and McCreanor, 1985). Indeed, KYNA production in the rat brain was saturable only
364 at high L-KYN (≈1 mM) concentration (Turski et al., 1989), which is concordant with our
365 findings.
366 In conclusion, mouse brain tissue intensively liberates endogenous and *de novo* synthesized
367 KYNA into the extracellular milieu *in vitro*, whereas the retained KYNA in the tissue is
368 negligible.

369 **4.3 Effect of KAT-2 inhibitor PF-04859989 on *de novo* KYNA release**

370 The advent of highly specific KAT-2 inhibitors opened new perspectives in clarifying KP
371 function in rodents (Dounay et al., 2012, Nematollahi et al., 2016). However, no
372 pharmacological experiment has yet targeted the mouse KAT-2 function, probably because of
373 its proposed irrelevance (Guidetti et al., 2007). In our previous anatomical study, we found
374 prominent KAT-2 immunopositivity in astrocytes and in GABAergic cells in the adult mouse
375 brain (Heredi et al., 2017). We therefore hypothesized that KAT-2 has a specific role in
376 mouse brain KYNA function. Because of the low basal KYNA content of the tissue
377 homogenate and that of the aCSF (usually close to the detection limit of HPLC), we estimated
378 the effect of the inhibitor on the KYN induced *de novo* KYNA production.
379 Applying the highly specific KAT-2 inhibitor PF-04859989 in a similar concentration, which
380 was found in the rat CSF after parenteral application (Dounay et al., 2012), resulted in a
381 decrease of *de novo* KYNA production by almost 40%. Although, this is higher than has
382 previously been reported using alternative methods, KYNA production was not completely
383 abolished following KAT-2 inhibition; 60% of total KAT activity remained. This indicates
384 that, in a whole other KAT enzymes make a greater contribution in the mouse brain, however,
385 it does not exclude the important role of mouse KAT-2. Indeed, an incomplete inhibition of
386 KAT activity is more suitable in the experimental models of therapeutical KYNA level
387 reduction. Our results indicate that the investigation of the effects of pharmacological KAT-2
388 inhibition should be extended to mouse models, which was largely neglected in this relation.
389

390 **Acknowledgments**
391 Thanks are due to Matthew Higginson for grammar proofreading.
392

393 **Funding**
394 This study was supported by grant GINOP 2.3.2-15-2016-00034 and co-financed by EFOP-
395 3.6.1-16-2016-00008 grant and grant by MTA-SZTE Neuroscience Research group. LG, JH,

JT, ZsK, LV, EO were fellows in the JSPS-HAS mobility scholarship program (NKM-48/2017). Dénes Zádori was supported by the János Bolyai Scholarship of the Hungarian Academy of Sciences.

Conflict of interest

The authors declare no competing financial interests. All co-author agree with the submission of this form of the manuscript.

5 References

Albuquerque EX, Schwarcz R (2013) Kynurenic acid as an antagonist of alpha7 nicotinic acetylcholine receptors in the brain: facts and challenges. Biochem Pharmacol 85:1027-1032.

Alexander KS, Wu HQ, Schwarcz R, Bruno JP (2012) Acute elevations of brain kynurenic acid impair cognitive flexibility: normalization by the alpha7 positive modulator galantamine. Psychopharmacology (Berl) 220:627-637.

Alkondon M, Pereira EF, Eisenberg HM, Kajii Y, Schwarcz R, Albuquerque EX (2011) Age dependency of inhibition of alpha7 nicotinic receptors and tonically active N-methyl-D-aspartate receptors by endogenously produced kynurenic acid in the brain. J Pharmacol Exp Ther 337:572-582.

Alkondon M, Pereira EF, Todd SW, Randall WR, Lane MV, Albuquerque EX (2015) Functional G-protein-coupled receptor 35 is expressed by neurons in the CA1 field of the hippocampus. Biochem Pharmacol 93:506-518.

Alkondon M, Pereira EF, Yu P, Arruda EZ, Almeida LE, Guidetti P, Fawcett WP, Sapko MT, Randall WR, Schwarcz R, Tagle DA, Albuquerque EX (2004) Targeted deletion of the kynurenine aminotransferase ii gene reveals a critical role of endogenous kynurenic acid in the regulation of synaptic transmission via alpha7 nicotinic receptors in the hippocampus. J Neurosci 24:4635-4648.

Amaral M, Outeiro TF, Scrutton NS, Giorgini F (2013) The causative role and therapeutic potential of the kynurenine pathway in neurodegenerative disease. Journal of molecular medicine 91:705-713.

Artru A.A. (1993) Cerebrospinal Fluid: Physiology and Pharmacology. In: Sperry R.J., Johnson J.O., Stanley T.H. (eds) Anesthesia and the Central Nervous System. Developments in Critical Care Medicine and Anesthesiology, vol 28. Springer, Dordrecht

Banerjee J, Alkondon M, Albuquerque EX (2012a) Kynurenic acid inhibits glutamatergic transmission to CA1 pyramidal neurons via alpha7 nAChR-dependent and -independent mechanisms. Biochem Pharmacol 84:1078-1087.

Banerjee J, Alkondon M, Pereira EF, Albuquerque EX (2012b) Regulation of GABAergic inputs to CA1 pyramidal neurons by nicotinic receptors and kynurenic acid. J Pharmacol Exp Ther 341:500-509.

Bender DA, McCreanor GM (1985) Kynurenine hydroxylase: a potential rate-limiting enzyme in tryptophan metabolism. Biochem Soc Trans 13:441-443.

Berlinguer-Palmini R, Masi A, Narducci R, Cavone L, Maratea D, Cozzi A, Sili M, Moroni F, Mannaioni G (2013) GPR35 activation reduces Ca2+ transients and contributes to the kynurenic acid-dependent reduction of synaptic activity at CA3-CA1 synapses. PLoS One 8:e82180.

Birch PJ, Grossman CJ, Hayes AG (1988) Kynurenic acid antagonises responses to NMDA via an action at the strychnine-insensitive glycine receptor. Eur J Pharmacol 154:85-87.

Buskila Y, Breen PP, Tapson J, van Schaik A, Barton M, Morley JW (2014) Extending the viability of acute brain slices. Scientific reports 4:5309.

Cho S, Wood A, Bowlby MR (2007) Brain slices as models for neurodegenerative disease and screening platforms to identify novel therapeutics. Curr Neuropharmacol 5:19-33.

Chuquet J, Quilichini P, Nimchinsky EA, Buzsaki G (2010) Predominant enhancement of glucose uptake in astrocytes versus neurons during activation of the somatosensory cortex. J Neurosci 30:15298-15303.

Davolio C, Greenamyre JT (1995) Selective vulnerability of the CA1 region of hippocampus to the indirect excitotoxic effects of malonic acid. Neurosci Lett 192:29-32.

Dounay AB, Anderson M, Bechle BM, Campbell BM, Claffey MM, Evdokimov A, Evrard E, Fonseca KR, Gan X, Ghosh S, Hayward MM, Horner W, Kim JY, McAllister LA, Pandit J, Paradis V, Parikh VD, Reese MR, Rong S, Salafia MA, Schuyten K, Strick CA, Tuttle JB, Valentine J, Wang H, Zawadzke LE, Verhoest PR (2012) Discovery of Brain-Penetrant, Irreversible Kynurenine Aminotransferase II Inhibitors for Schizophrenia. ACS medicinal chemistry letters 3:187-192.

457 Dounay AB, Tuttle JB, Verhoest PR (2015) Challenges and Opportunities in the Discovery of New
458 Therapeutics Targeting the Kynurenine Pathway. J Med Chem 58:8762-8782.
459 Fujigaki S, Saito K, Takemura M, Fujii H, Wada H, Noma A, Seishima M (1998) Species differences in L-
460 tryptophan-kynurenine pathway metabolism: quantification of anthranilic acid and its
461 related enzymes. Arch Biochem Biophys 358:329-335.
462 Fukuda A, Czurko A, Hida H, Muramatsu K, Lenard L, Nishino H (1995) Appearance of deteriorated
463 neurons on regionally different time tables in rat brain thin slices maintained in physiological
464 condition. Neurosci Lett 184:13-16.
465 Gal EM, Sherman AD (1980) L-kynurenine: its synthesis and possible regulatory function in brain.
466 Neurochem Res 5:223-239.
467 Guidetti P, Amori L, Sapko MT, Okuno E, Schwarcz R (2007) Mitochondrial aspartate
468 aminotransferase: a third kynurenate-producing enzyme in the mammalian brain. J
469 Neurochem 102:103-111.
470 Han Q, Cai T, Tagle DA, Li J (2010a) Structure, expression, and function of kynurenine
471 aminotransferases in human and rodent brains. Cellular and molecular life sciences : CMLS
472 67:353-368.
473 Han Q, Cai T, Tagle DA, Li J (2010b) Thermal stability, pH dependence and inhibition of four murine
474 kynurenine aminotransferases. BMC Biochem 11:19.
475 Heredi J, Berko AM, Jankovics F, Iwamori T, Iwamori N, Ono E, Horvath S, Kis Z, Toldi J, Vecsei L,
476 Gellert L (2017) Astrocytic and neuronal localization of kynurenine aminotransferase-2 in the
477 adult mouse brain. Brain Struct Funct 222:1663-1672.
478 Hodgkins PS, Wu HQ, Zielke HR, Schwarcz R (1999) 2-Oxoacids regulate kynurenic acid production in
479 the rat brain: studies in vitro and in vivo. J Neurochem 72:643-651.
480 Kovalenko T, Osadchenko I, Nikonenko A, Lushnikova I, Voronin K, Nikonenko I, Muller D, Skibo G
481 (2006) Ischemia-induced modifications in hippocampal CA1 stratum radiatum excitatory
482 synapses. Hippocampus 16:814-825.
483 Lein PJ, Barnhart CD, Pessah IN (2011) Acute hippocampal slice preparation and hippocampal slice
484 cultures. Methods Mol Biol 758:115-134.
485 Lundgaard I, Li B, Xie L, Kang H, Sanggaard S, Haswell JD, Sun W, Goldman S, Blekot S, Nielsen M,
486 Takano T, Deane R, Nedergaard M (2015) Direct neuronal glucose uptake heralds activity-
487 dependent increases in cerebral metabolism. Nature communications 6:6807.
488 Miller JM, MacGarvey U, Beal MF (1992) The effect of peripheral loading with kynurenine and
489 probenecid on extracellular striatal kynurenic acid concentrations. Neurosci Lett 146:115-
490 118.
491 Moroni F, Russi P, Lombardi G, Beni M, Carla V (1988) Presence of kynurenic acid in the mammalian
492 brain. J Neurochem 51:177-180.
493 Nematollahi A, Sun G, Jayawickrama GS, Church WB (2016) Kynurenine Aminotransferase Isozyme
494 Inhibitors: A Review. International journal of molecular sciences 17.
495 Okuno A, Fukuwatari T, Shibata K (2011) High tryptophan diet reduces extracellular dopamine
496 release via kynurenic acid production in rat striatum. J Neurochem 118:796-805.
497 Olsson SK, Larsson MK, Erhardt S (2012) Subchronic elevation of brain kynurenic acid augments
498 amphetamine-induced locomotor response in mice. J Neural Transm (Vienna) 119:155-163.
499 Potter MC, Elmer GI, Bergeron R, Albuquerque EX, Guidetti P, Wu HQ, Schwarcz R (2010) Reduction
500 of endogenous kynurenic acid formation enhances extracellular glutamate, hippocampal
501 plasticity, and cognitive behavior. Neuropsychopharmacology 35:1734-1742.
502 Prescott C, Weeks AM, Staley KJ, Partin KM (2006) Kynurenic acid has a dual action on AMPA
503 receptor responses. Neurosci Lett 402:108-112.
504 Rosenthal N, Brown S (2007) The mouse ascending: perspectives for human-disease models. Nature
505 cell biology 9:993-999.
506 Scharfman HE, Hodgkins PS, Lee SC, Schwarcz R (1999) Quantitative differences in the effects of de
507 novo produced and exogenous kynurenic acid in rat brain slices. Neurosci Lett 274:111-114.

Schwieler L, Erhardt S, Nilsson L, Linderholm K, Engberg G (2006) Effects of COX-1 and COX-2 inhibitors on the firing of rat midbrain dopaminergic neurons--possible involvement of endogenous kynurenic acid. Synapse 59:290-298.

Swartz KJ, During MJ, Freese A, Beal MF (1990) Cerebral synthesis and release of kynurenic acid: an endogenous antagonist of excitatory amino acid receptors. J Neurosci 10:2965-2973.

Turski WA, Gramsbergen JB, Traitler H, Schwarcz R (1989) Rat brain slices produce and liberate kynurenic acid upon exposure to L-kynurenine. J Neurochem 52:1629-1636.

Urbanska EM, Chmielewski M, Kocki T, Turski WA (2000) Formation of endogenous glutamatergic receptors antagonist kynurenic acid--differences between cortical and spinal cord slices. Brain Res 878:210-212.

Vecsei L, Szalardy L, Fulop F, Toldi J (2013) Kynurenines in the CNS: recent advances and new questions. Nature reviews Drug discovery 12:64-82.

Zmarowski A, Wu HQ, Brooks JM, Potter MC, Pellicciari R, Schwarcz R, Bruno JP (2009) Astrocyte-derived kynurenic acid modulates basal and evoked cortical acetylcholine release. Eur J Neurosci 29:529-538.

525 ## Legend to figures

526 **Fig. 1: Glucose consumption in the course of 4h SV incubation.** Acute slices were
527 incubated as routinely in aCSF having high glucose concentration (10mM). Glucose
528 concentration was already dropped after 30 min (≈8%), however, the decrease was not
529 statistically significant (F=4,281; p=0,072; Partial Eta Squared: 0,349). 4h incubation,
530 however, resulted in a significant decrease of aCSF glucose content (≈20%) (F=20,304;
531 p=0,002; Partial Eta Squared: 0,717). Data are expressed as a percentage of baseline glucose
532 content (glucose content of the aCSF at the starting point of the experiment) and represent the
533 mean ± SD. n=5 animals, 6+6 corresponding brain slices per condition.
534

535 **Fig. 2: LDH release in the course of 4h SV incubation.** At the beginning of the incubation
536 aCSF LDH content is virtually zero (only measuring error is depicted). In comparison,
537 gradual increase of the aCSF LDH content could be measured in the course of 30 min (Z=
538 16,910; p= 0,959) and 4h incubation (Z= 16,910; p=0,030). However Triton X-100 treatment
539 resulted in a ≈14 fold increase of LDH in the aCSF after 4h (Z= 16,910; p=0,001). This
540 indicates that the cell membrane integrity is largely preserved in the case of 4h incubation.
541 Data represent the mean ± SD. n=9 animals, 6+6 corresponding brain slices per condition.
542

543 **Fig. 3: Cresyl violet staining (A-B) and NeuN immunolabelling (C-D) in the dorsal**
544 **hippocampus of mouse acute brain slices.** There was no visible difference between the LV
545 **(A-C)** and SV **(B-D)** group in the CA1 area of the hippocampus after 4h incubation. Cells
546 keep their normal appearing in the pyramidal cell layer. Scale bars are 100 µm.

547 **Fig. 4: Basal glutamatergic synaptic properties of acute brain slices.** There is no
548 significant difference between slices recorded immediately after post-slicing recovery period
549 (30 min.), or incubated under LV condition for 4hours and under SV conditions, respectively
550 (F=0.793; p=0,465; Partial Eta Squared: 0,064). The values represent normalized means±SD
551 and were plotted as a function of stimulus strength. n=17 animals; 11+9+8 recordings/group.

552 **Fig. 5: Basal and *de novo* KYNA content in the incubating aCSF and in the tissue**
553 **homogenate after 4h incubation.** Without L-KYN administration 7.01±2.03ng basal KYNA
554 content could be measured from the aCSF and 0.22±0.07ng from the brain tissue homogenate.
555 In contrast, as a result of 10 µM L-KYN administration we found a 6.3 fold increase in the
556 aCSF (44.56 ±6,99ng) (Z=6,818; p= 0,009) and a 3.8 fold increase in the tissue (0.85±0.21ng)
557 KYNA content. The values represent means ±SD. n=5 animals, 6+6 corresponding brain
558 slices per condition.

559 **Fig. 6: Effect of KAT-2 inhibitor PF-04859989 on de novo KYNA release.** Acute slices
560 were incubated in the presence of 10µM L-KYN with or without PF-04859989 in a
561 concentration of 5µM. KYNA content of the aCSF was measured after 4h incubation. High
562 KYNA content could be measured in the L-KYN group (55.19±6.45ng). Addition of the
563 inhibitor resulted in a significant decrease of the released KYNA in the aCSF by almost 40%
564 (34.5±6.93ng; F=23,868; p=0,001; Partial Eta Squared: 0,749). The values represent
565 means±SD. n=5 animals, 6+6 corresponding brain slices per condition.

566

Highlights for the manuscript entitled:

Investigating KYNA production and kynurenergic manipulation on acute mouse brain slice preparations

a) Acute brain slices are functional after incubation in low bulk volume of aCSF.

b) Mouse brain slices release the majority of kynurenic acid into incubating aCSF.

c) Kynurenic acid release is elevated after L-kynurenine supplementation.

d) Kynurenine aminotransferase-2 inhibitor reduces kynurenic acid release.

Investigating KYNA production and kynurenergic manipulation on acute mouse brain slice preparations

Judit Herédi[1], Edina Katalin Cseh[2], Anikó Magyariné Berkó[1], Gábor Veres[2], Dénes Zádori[2], József Toldi[1], Zsolt Kis[1],László Vécsei[2,3],Etsuro Ono[4];Levente Gellért[1,5,*]

[1]Department of Physiology, Anatomy and Neuroscience, Faculty of Science and Informatics, University of Szeged, Közép Fasor 52., Szeged 6726, Hungary.

[2]Department of Neurology, Faculty of Medicine, University of Szeged, Semmelweis st.6, Szeged 6725 Hungary

[3]MTA-SZTE Neuroscience Research Group, University of Szeged, Semmelweis st. 6, Szeged 6725, Hungary.

[4]Department of Biomedicine, Graduate School of Medical Sciences, Kyushu University Fukuoka, Japan; Center of Biomedical Research, Research Center for Human Disease Modeling, Graduate School of Medical Sciences, Kyushu University Fukuoka, Japan.

[5]Institute of Physiology, University Medical Center of the Johannes Gutenberg University Mainz, Duesbergweg 6, D-55128 Mainz, Germany.

[*]Correspondence: Levente Gellért,
Institute of Physiology, University Medical Center of the Johannes Gutenberg University Mainz, Duesbergweg 6, D-55128 Mainz, Germany.

Abstract

Manipulation of kynurenic acid (KYNA) level through kynurenine aminotransferase-2 (KAT-2) inhibition with the aim of therapy in neuro-psychiatric diseses has been the subject of extensive recent research. Although mouse models are of particular importance, neither the basic mechanism of KYNA production and release nor the relevance of KAT-2 in the mouse brain has yet been clarified.

Using acute mouse brain slice preparations, we investigated the basal and L-kynurenine (L-KYN) induced KYNA production and distribution between the extracellular and intracellular compartments. Furthermore, we evaluated the effect of specific KAT-2 inhibition with the irreversible inhibitor PF-04859989. To ascertain that the observed KYNA release is not a simple consequence of general cell degradation, we examined the structural and functional integrity of the brain tissue with biochemical, histological and electrophysiological tools.

We did not find relevant change in the viability of the brain tissue after several hours incubation time. HPLC measurements proved that mouse brain slices intensively produce and liberate KYNA to the extracellular compartment, while only a small proportion retained in the tissue both in the basal and L-KYN supplemented state. Finally, specific KAT-2 inhibition significantly reduced the extracellular KYNA content.

Taken together, these results provide important data about KYNA production and release, and *in vitro* evidence for the first time of the function of KAT-2 in the adult mouse brain. Our study extends investigations of KAT-2 manipulation to mice in a bid to fully understand the function; the final, future aim is to assign therapeutical kynurenergic manipulation strategies to humans.

Keywords: kynurenic acid, kynurenine aminotransferase-2 inhibition; acute slice viability; HPLC; immunohistochemistry; in vitro electrophysiology

Investigating KYNA production and kynurenergic manipulation on acute mouse brain slice preparations

Judit Herédi[1], Edina Katalin Cseh[2], Anikó Magyariné Berkó[1], Gábor Veres[2], Dénes Zádori[2], József Toldi[1], Zsolt Kis[1],László Vécsei[2,3],Etsuro Ono[4];Levente Gellért[1,*]

[1]Department of Physiology, Anatomy and Neuroscience, Faculty of Science and Informatics, University of Szeged, Közép Fasor 52., Szeged 6726, Hungary.

[2]Department of Neurology, Faculty of Medicine, University of Szeged, Semmelweis st.6, Szeged 6725 Hungary

[3]MTA-SZTE Neuroscience Research Group, University of Szeged, Semmelweis st. 6, Szeged 6725, Hungary.

[4]Department of Biomedicine, Graduate School of Medical Sciences, Kyushu University Fukuoka, Japan; Center of Biomedical Research, Research Center for Human Disease Modeling, Graduate School of Medical Sciences, Kyushu University Fukuoka, Japan.

[*]Correspondence: Levente Gellért, Department of Physiology, Anatomy and Neuroscience, University of Szeged, Közép fasor 52, Szeged, H-6726, Hungary
e-mail: gellert.levente1@gmail.com

Keywords: kynurenic acid, kynurenine aminotransferase-2 inhibition; acute slice viability; HPLC; immunohistochemistry; in vitro electrophysiology

1 Introduction

Tryptophan (TRP) is catabolized mostly through the kynurenine pathway (KP) in the mammalian brain (Gal and Sherman 1980). Kynurenic acid (KYNA) is one of the neuroactive products of this metabolic route. KYNA is synthesized with the irreversible transamination of L-kynurenine (L-KYN), a reaction catalyzed by kynurenine aminotransferases (KATs) (Han et al., 2010a). KYNA exerts multiple effects on ligand-gated ion channels (Gal and Sherman, 1980, Birch et al., 1988, Prescott et al., 2006, Albuquerque and Schwarcz, 2013) and on the G-protein-coupled receptor 35 in the brain (Berlinguer-Palmini et al., 2013, Alkondon et al., 2015). Through these actions, KYNA can modulate neurotransmission systems (Zmarowski et al., 2009, Alexander et al., 2012, Banerjee et al., 2012a, Olsson et al., 2012). Indeed, the role of KYNA in neurophysiological and neuropathological processes has been the subject of extensive contemporary studies. The causal role of diversion of the KP has been proposed in several neurodegenerative and neuropsychiatric disorders (e.g. Alzheimer's disease, Parkinson's disease, Huntington's disease, cerebral ischemia, depression, and schizophrenia) (Vecsei et al., 2013). Thus, kynurenergic manipulation with the aim of therapy has also been proposed (Amaral et al., 2013).

To date, cross-species differences of the relevance and regulation of brain KP function and KYNA production are not fully clarified. The majority of the experimental data concerns the rat kynurenine system, however, mouse models are of particular importance as well (Rosenthal and Brown, 2007).

Yet, there is neither detailed study about the mechanism and regulation of KYNA release from cells in the mouse brain parenchyma, nor information about the function of relevant KAT enzymes of the KP. For instance, the importance of kynurenine aminotransferase-2 (KAT-2) in the rat and human brain is unequivocal, the relevance of KAT-2 in the mouse brain is, however, controversial (Han et al., 2010a).

For describing the kynurenine system in model animals and investigating the effect of kynurenergic manipulation, *in vitro* models are essential and complement *in vivo* studies. To this end, acute brain slice preparations provide many advantages over *in vivo* experiments (Cho et al., 2007, Lein et al., 2011). Previously, KYNA production and release to the extracellular compartment upon L-KYN exposure was described in cortical (Turski et al., 1989, Hodgkins et al., 1999) and in hippocampal rat brain slices (Scharfman et al., 1999, Alkondon et al., 2011). However, there is no data about KYNA production of acute mouse brain slice preparations. Furthermore, these studies did not concern the acute slice viability, a factor, which can strongly influence the KYNA production and release.

55 The present study was designed to estimate the KYNA production and release of acute mouse
56 brain slices and to assess the effect of the specific KAT-2 inhibitor PF-04859989 on KYNA
57 production *in vitro.*
58 Basing on literature data we presumed that the concentration of KYNA released into the
59 extracellular space falls into the picomolar or low nanomolar range (Schwieler et al., 2006).
60 To ensure a measurable concentration of KYNA for HPLC assessments we incubated our
61 slices in a low bulk volume of artificial cerebrospinal fluid (aCSF) (that is approx. 6 ml of
62 aCSF/100mg wet weight brain tissue) under continuous carbogenation, but without perfusion.
63 In previous studies KYNA increase and release could be measured 2-4hours after L-KYN
64 administration in rat (Turski et al., 1989, Swartz et al., 1990). Results of our pilot experiments
65 are in line with that finding (unpublished data). Therefore, we decided to incubate brain slices
66 for 4-6 hours. Incubation of acute slices inherently initiates progressive damage in the tissue
67 (Fukuda et al., 1995). It is therefore possible that metabolic properties and integrity of cells
68 involved in KYNA production and release might alter during several hours of incubation. In
69 order to characterize the after-incubation viability of the brain tissue we performed
70 histological observations, biochemical and electrophysiological characterization of the slices.
71 To investigate the extra/intracellular distribution of basal KYNA, we compared the KYNA
72 content in the tissue with that liberated into the extracellular space. Then, we wanted to know
73 if we could induce *de novo* KYNA production with the administration of the KYNA precursor
74 L-KYN. Finally, we investigated the effect of the KAT-2 inhibitor on the L-KYN-induced
75 KYNA release.
76 Investigating tissue viability, we found a slight alteration in some of the observed tissue
77 viability measures. However, the slices showed no anatomical or functional abnormalities, so
78 tissue integrity was preserved.
79 Regarding KYNA production, we found that in the course of 4hours incubation slices readily
80 release both basal and *de novo* produced KYNA into the supernatant aCSF, whereas only a
81 negligible fraction of total KYNA is retained in the tissue. The KAT-2 inhibitor, however,
82 conspicuously decreased KYNA release.
83

2 Experimental Procedures

2.1 Animals

8-12 weeks old male *C57Bl/6* mice obtained from The National Institute of Oncology (Budapest, Hungary) were used (n=30) for the experiments. Animals were kept under controlled laboratory conditions and had free access to food and water. All experiments were in compliance with the guidelines of the European Communities Council Directives (2010/63/EU) and the Hungarian Act for the Protection of Animals in Research (XXVIII.tv. 32.§).

2.2 Acute slice preparation

Animals were anesthetized with isoflurane (3%) followed by decapitation (NEMI Guillotine; Braintree Scientific, Inc.). The brain was rapidly removed and submerged in ice-cold aCSF (pH 7.4) composed of (in mM): 234 sucrose, 3.5 KCl, 1 NaH_2PO_4, 24 $NaHCO_3$, 1 $CaCl_2$, 3 $MgSO_4$ and 10 D-glucose (Sigma Aldrich) and oxygenated with 95% O_2 and 5% CO_2. 350 µm thick sections were obtained with a vibratome (Leica VT1200S, Germany); the two hemispheres were dissected and transferred to a holding chamber. Slices were allowed to recover for 30 min in aCSF (pH 7.4) containing (in mM): 130 NaCl, 3.5 KCl, 1 NaH_2PO_4, 24 $NaHCO_3$, 1.5 $CaCl_2$, 3 $MgSO_4$ and 10 D-glucose

2.3 Small volume incubation of brain slices

After 30 min recovering, one hemisphere of the 6 coronal slices were transferred to the incubation chambers containing a low bulk volume of aCSF (appr. 6ml of aCSF/6 half coronal slice), placed on a closed-loop temperature controller pad (TMP-5b, Supertech Instruments UK Ltd.) at 30 °C to reach optimal temperature for KAT function (Banerjee et al., 2012b) **(SV condition hereafter)**. The aCSF was continuously bubbled with 95% O_2 and 5% CO_2 but was not circulated during the incubation.

For comparison of tissue viability of slices incubated in SV condition or in standard condition, we performed the same battery of experiments on the corresponding 6 half coronal slices kept under standard conditions (high bulk volume of aCSF; ≈200ml/6 half coronal slice) at 20 °C **(LV condition hereafter)**. Through this LV slice incubation routine we could perform stable field excitatory postsynaptic potentials (fEPSP) recordings after 8h incubation, therefore, this condition was used as an adequate control for assessing tissue viability under SV condition.

115 After evaluating tissue viability, we studied KYNA production and kynurenergic
116 manipulation in the SV condition. 10 µM L-KYN (Sigma Aldrich) and 5 µM KAT-2 inhibitor
117 PF-04859989 were dissolved in aCSF. The scheme of the protocol used in this study is
118 illustrated in **Supp. Fig. 1.**
119 At the end of the incubations, the supernatants were collected and stored at -80 °C for further
120 biochemical analysis. One portion of the slices were placed in 4% paraformaldehyde (PFA)
121 and fixed overnight for histological studies, whereas the remaining slices were immediately
122 frozen in liquid nitrogen and stored at -80 °C for Western blotting (see in the supplement).

123 **2.4 Electrophysiology**

124 After 4h incubation in the LV or SV condition, the slices were transferred to an interface
125 recording chamber and superfused with aCSF containing (in mM): 130 NaCl, 3.5 KCl, 1
126 $NaH2PO_4$, 24 $NaHCO_3$, 3 $CaCl_2$, 1.5 $MgSO_4$ and 10 D-glucose. The temperature (32 °C) and
127 flow rate (2 ml/min) of the aCSF were continuously controlled. Baseline synaptic function of
128 the tissue was tested with input-output (I/O) curve recordings on the CA3-CA1 cell synapses
129 in the hippocampus. Schaffer collaterals were stimulated at 0,05 Hz using a concentric bipolar
130 stainless steel electrode (Neuronelektrod Ltd, Hungary). fEPSPs were recorded from the
131 stratum radiatum of CA1 region with 1,5–3 mOhm resistance glass microelectrodes.
132 Potentials were amplified and filtered with WPI AMP-04 amplifier and digitalized with Axon
133 Digidata 1320A. Recordings were monitored and saved with Axoscope 10.0 (Molecular
134 Devices Corporation, USA). Data were analyzed with Clampfit 10.6 (Molecular Devices,
135 USA) and OriginPro 8.6 (OriginLab Corporation, USA) softwares. In the course of I/O curve
136 recordings to define the minimal stimulus we decreased the stimulus intensity until minimal
137 but unequivocal fEPSP was evoked. The stimulus was then increased in 5 µA increments. We
138 collected five responses and averaged at each increment. We continued to increase the
139 stimulus intensity until fEPSP response had saturated. fEPSP slope values were normalized
140 and averaged across all slices in each group and plotted as a function of normalized stimulus
141 intensity to construct I/O curves.

142 **2.5 Histology**

143 Fixed brain slices were cryoprotected with sucrose solution and 30 µm thick sections were cut
144 with a freezing microtome (Reichert-Jung 1206).
145 *Immunohistochemistry:* Free-floating sections were washed in PBT, incubated in 1% NDS
146 and exposed to the primary antibody (mouse anti-NeuN, 1:4000, Millipore) overnight at 4 °C.

147 Next day, they were incubated in the appropriate secondary antibody (1:500; Jackson
148 ImmunoResearch) at room temperature. Primary and secondary antibody were diluted in 0.1
149 M PBT containing 1% NDS. Negative control was prepared from sections incubated without
150 the primary antibody. The sections were coverslipped with antifade mounting medium
151 (ProLong® Gold, Life Technologies).
152 *Cresyl violet staining:* We performed cresyl violet staining for morphological observations
153 after different incubation conditions and time. Sections were rehydrated with descending
154 grades of alcohol and stained with cresyl violet staining solution for 5 min. After staining,
155 samples were passed through ascending alcohol solutions and immersed in xylene for 5 min.
156 Sections were coverslipped with Entallan®.
157 All photomicrographs were obtained with an Olympus BX51 microscope fitted with a DP70
158 digital imaging system.

159 **2.6 Lactate dehydrogenase (LDH) assay**

160 For evaluating tissue viability we performed LDH activity assay on supernatant samples
161 collected after 30 min, 4h and 6 h incubation time. As positive control for LDH release we
162 permeabilized the cell membrane with Triton X-100™ (1%). LDH activity was measured at
163 340 nm and 37 ˚C using an LDH activity assay kit (Diagnosticum Ltd, Hungary, 46461) on a
164 BioLis 24i Premium system (Siemens). LDH activity was expressed as U/l/100 mg tissue.

165 **2.7 Hexokinase (HK) assay**

166 Glucose content was measured by HK activity assay on supernatant samples collected after 30
167 min, 4h and 6h incubation time. HK activity was measured at 340 nm and 37 ˚C using a two-
168 step Glu HK activity assay kit (Diagnosticum Ltd, Hungary, 47361) on a BioLis 24i Premium
169 system (Siemens).

170 **2.8 High performance liquid chromatography (HPLC)**

171 The brain slices were weighed and then homogenized for 30s in 250 ml ice-cold solution,
172 containing trifluoroacetic acid (0.1% v/v) and 2 µM 3-nitro-L-tyrosine (3-NLT, as internal
173 standard). The homogenate was centrifuged at 12000 RPM for 10 min at 4°C. The
174 supernatants were stored at -80°C until further analysis. Similar procedure was applied for the
175 aCSF samples, briefly, 250 µL aCSF was treated with 50 µl of above-mentioned solution, and
176 then centrifuged under the same circumstances as the brain tissues. The resulting supernatants
177 were measured with an Agilent 1100 HPLC system (Agilent Technologies, Santa Clara, CA,
178 USA) combined with a fluorescence (FLD) and a UV detector. For the determination of

179 KYNA, the excitation and emission wavelengths of FLD were set at 344 nm and 398 nm,
180 whereas the UV detector was set at 365 nm for the determination of 3-NLT. Chromatographic
181 separations were performed on an a Kinetex C18 column, 150 x 4.6 mm I.D., 5 µm particle
182 size (Phenomenex Inc., Torrance, CA, USA) preceded by Security Guard pre-column C18, 4
183 x 3.0 mmI.D., 5 µm particle size (Phenomenex Inc., Torrance, CA, USA) with a mobile phase
184 composition of 0.2 M zinc acetate/ACN = 95/5 v/v%, in which pH was adjusted at 6.2 with
185 acetic acid, applying isocratic elution. The flow rate was 1.2 ml/min and the injection volume
186 was 50 µL. As for the method validation, following parameters are reported, briefly,
187 regarding KYNA in tissue and aCSF. The LOD and LOQ in tissue and aCSF samples were 1
188 and 3.75 nM, respectively. With regard to precision, the relative standard deviation was ≤
189 2.2%. The recoveries in tissue and aCSF samples ranged from 103% to 108% and 81% to
190 91%, respectively.

191 **2.9 Data analysis and Statistics**

192 KYNA content was calculated from the concentration values measured by HPLC and data
193 were normalized to the tissue weight. In the case of the aCSF, values represented KYNA
194 content released by 100 mg tissue. LDH release and glucose consumption data were similarly
195 normalized to 100 mg tissue.
196 All statistical computations were carried out with the IBM SPSS Statistics software (version
197 20.). Homogeneity of variance across groups was tested with the Levene's Test of Equality of
198 Error Variances. Distribution of the data was tested with the-Shapiro-Wilk test of normality.
199 Statistical significance was calculated with the GLM univariate model. If assumption of
200 variance homogeneity was violated, Kruskal-Wallis Test was used. For repeated measures of
201 the I/O curve recordings, General Linear Model Repeated Measures method was applied.
202

3 Results

3.1 Glucose consumption

To our best knowledge, there is no literature data about the minimal bulk volume of aCSF in which acute mouse brain slices can function quasi normally for hours. Therefore, first, we asked if the glucose availability in the aCSF under SV condition exceeds the nutrition demand of the slices.

Glucose consumption measurement proved that glucose availability gradually decreased during the incubation. Glucose concentration was already dropped after 30 min, however, the decrease was not statistically significant (F=4,281; p=0,072; Partial Eta Squared: 0,349). 4h incubation, however, resulted in a significant decrease of aCSF glucose content (F=20,304; p=0,002; Partial Eta Squared: 0,717) compared to original level (**Fig. 1).** It was further declined during the 6h incubation time (data not depicted).

3.2 Viability of acute brain slices – LDH release

A characteristic sign of the perturbation of normal cellular function is the loss of cell membrane integrity and the concomitant increase of membrane permeability (Cho et al., 2007). Therefore, alteration in LDH release to the extracellular space is a sensitive measure of cell viability. Under SV condition LDH release was continuously increasing in the aCSF during 30 min (Z= 16,910; p=0,959), 4h (Z= 16,910; p=0,030) and also 6 h incubation (data not depicted), compared to the initial state. However, Triton X-100 treatment resulted in a ≈14 fold increase of LDH in the aCSF after 4h incubation (Z= 16,910; p=0,001) **(Fig. 2)**. This indicates that the cell membrane integrity is largely preserved in the course of 4h incubation. The observed KYNA release is not the simple consequence of disrupted membrane integrity (see below).

3.3 Histological observations

For the histological examination of tissue state we performed NeuN immunolabelling and cresyl violet staining. There was no visible tissue damage in the vulnerable CA1 subregion of the dorsal hippocampus. CA1 pyramidal cell shape and size appeared normal after 4h incubation **(Fig. 3)**. However, the structural integrity of pyramidal cells in CA1 was not completely preserved after 6h incubation. Compared to the control group, shrunken and deformed pyramidal cells emerged (visual observation).

235 **3.4 Synaptic properties of acute brain slices - I/O curves**

236 Basal glutamatergic synaptic properties were tested by means of fEPSP recording, expressed
237 against gradually increased stimulating intensity in certain groups. There was no significant
238 difference between slices recorded immediately after post-slicing recovery period (30 min.),
239 or incubated under LV condition for 4hours and under SV conditions, respectively (F=0.793;
240 p=0,465; Partial Eta Squared: 0,064). This result indicates that, the baseline synaptic function
241 of the brain tissue was preserved after 4h SV incubation **(Fig. 4)**.

242 Considering the decreased glucose availability and increased LDH release, furthermore the
243 visually observed tissue damage after 6 h, the 4h long incubation duration was considered to
244 be the most suitable for KYNA measurement.

245 **3.5 KYNA production in mouse brain slices**

246 To examine whether mouse brain slices liberate endogenous and *de novo* produced KYNA
247 upon L-kynurenine administration during 4h long incubation period we performed HPLC
248 measurements from brain tissue homogenate and from incubating aCSF.
249 Without L-KYN administration 7.01±2.03ng basal KYNA content could be measured from
250 the aCSF and 0.22±0.07ng from the brain tissue homogenate. In contrast, as a result of 10 µM
251 L-KYN administration we found a 6.3 fold increase in the aCSF (44.56 ±6,99ng) (Z=6,818;
252 p=0,009) and a 3.8 fold increase in the tissue (0.85±0.21ng) KYNA content **(Fig. 5)**. No
253 considerable KYNA elevation could be observed in the course of 6h incubation compared to
254 the 4h incubation (data not depicted).
255 In conclusion, ≈97% of the total KYNA content was released to the extracellular
256 compartment (aCSF), whereas only ≈3% remained in the tissue under both conditions **(Supp.**
257 **Fig. 2)**

258 **3.6 Effect of KAT-2 inhibitor PF-04859989 on *de novo* KYNA release**

259 In the next series of experiments we incubated acute slices in the presence of 10 µM L-KYN,
260 with or without PF-04859989 in a concentration of 5µM. KYNA content of the aCSF was
261 measured after 4h incubation. Similar to former results high KYNA content could be
262 measured in the L-KYN group (55.19±6.45ng). Addition of the inhibitor resulted in a
263 significant decrease of the released KYNA in the aCSF by almost 40% (34.5±6.93ng;
264 F=23,868; p=0,001; Partial Eta Squared: 0,749) **(Fig. 6).**

4 Discussion

The implication of kynurenine metabolites in several brain disorders (e.g. schizophrenia, Alzheimer's disease, depression, migraine) shifted much attention to the manipulation of the KP in recent years (Dounay et al., 2015). The KP of tryptophan catabolism is present in many mammalian species (Moroni et al., 1988). Concomitantly, the neuromodulatory metabolites of this route are produced and function, making model animals suitable for extrapolating the effects of kynurenergic manipulation in humans. However, there are prominent differences among mammalian species regarding the kynurenine system (Moroni et al., 1988, Fujigaki et al., 1998), complicating further the understanding of the physiological and pathological role of the KP.

The physiological concentration of KYNA is different in model animals and in humans. The lowest basal KYNA level is found in the mouse brain, whereas it is the highest in the human neocortex (Moroni et al., 1988). The KYNA synthesizing enzyme isoforms have also a different role in different species. In the human and rat brain KAT-2 plays the major role in KYNA production, whereas in mice kynurenine aminotransferase-4 (KAT-4) was supposed to be the main KYNA synthesizing enzyme (Alkondon et al., 2004, Guidetti et al., 2007). However, KAT-2 null mutation resulted in the decrease of extracellular KYNA level in transgenic mice (Potter et al., 2010). Therefore, comparative characterization of the kynurenine catabolism in different model species is essential before assigning therapeutical kynurenergic manipulation strategies in humans.

Investigating the KP *in vitro* is of particular importance. In contrast to *in vivo* assays, acute brain slice preparations provide the possibility to exclude the perturbation effect of the peripheral KP function, while replicating or even changing many aspects of the *in vivo* context. A large panel of pharmacological interventions can be efficiently evaluated; furthermore, endogenous factors influencing brain KYNA production might also be easily clarified.

4.1 The after-incubation state of mouse brain slice preparations

One of the major limitations of acute brain slice models is the viability of nervous tissue, which endures on average for ≈ 6-8 hours (Buskila et al., 2014). However, there are specific brain areas (e.g. dorsal hippocampus) and cell populations where this window is even narrower (≈4hours) (Fukuda et al., 1995). To ascertain that KYNA release is not an uncontrolled function of a deteriorated brain tissue, we examined the after-incubation

viability. After 4h and 6h incubations in the SV aCSF, respectively, we observed slight alterations in tissue integrity and function.

The change of cell membrane integrity was evaluated by measuring the cytosolic LDH released into the aCSF. LDH could be measured and was continuously increasing during the incubation time, a phenomenon that verifies the limited and relatively narrow working window with acute brain slices. The considerably higher LDH content of the supernatant aCSF after membrane permeabilization indicates that after 4h incubation membrane integrity of the nervous tissue is largely preserved.

Changes in glucose consumption and glucose availability we estimated with a glucose hexokinase assay. We found that the available glucose was gradually decreased in the course of 4h and 6h incubation (not depicted). Although, continuous aCSF LDH level increase suggests a gradual loss of membrane integrity, decrease of glucose availability in the course of 4h and 6h incubation is possible only if, the nervous tissue actively metabolizes glucose. In the nervous tissue both astrocytic and neuronal glucose up-take is possible through facilitative membrane glucose transporters (Chuquet et al., 2010, Lundgaard et al., 2015). A shift toward one of these mechanisms we did not estimate, however we may conclude a generally preserved glucose up-take, consumption-machinery and functioning brain tissue.

Although the selective vulnerability of the CA1 region of the hippocampus to a variety of insults (e.g. excitotoxicity, cerebral ischemia) has been reported (Davolio and Greenamyre, 1995, Kovalenko et al., 2006) we observed no visible tissue damage in this brain area.

Furthermore, Schaffer-collateral CA1 pyramidal cell synapses were equally functional in the compared groups. There was no significant difference between slices recorded immediately after post-slicing recovery period (30 min.), or incubated under LV condition for 4hours and under SV conditions, respectively. This indicates that functional integrity of vulnerable region was largely preserved during a 4h SV incubation.

4.2 Basal and *de novo* KYNA production in mouse brain slices

Our first and basic question was, whether KYNA production can be measured and elevated in mouse brain slice preparations. To increase KYNA production L-KYN concentration (10 μM) was chosen on the basis of previous studies on slice preparations (Urbanska et al., 2000, Okuno et al., 2011). Similar to rat brain slices (Alkondon et al., 2011), mouse brain slices could produce KYNA upon L-KYN exposure and liberate newly formed KYNA to the extracellular space after 4h incubation **(See Fig. 5.)**. In trial experiments we measured KYNA production after 2h incubation, but there was no sufficient KYNA increase in the L-KYN

330 treated group on which the inhibition of KYNA synthesis could reliably be studied (not
331 depicted). Therefore, 4 h long incubation was necessary to examine KYNA production and
332 the effect of KAT-2 inhibition.
333 It is important to note that, extending the extracellular space of the acute slices with the
334 incubating aCSF (approx. 100 mg wet weight brain tissue/6ml aCSF) results in a considerably
335 smaller intracellular/extracellular volume ratio than found in the intact mouse brain (approx.
336 500mg wet weight brain tissue/0,04ml CSF (Artru, 1993). That difference means a steep
337 concentration gradient and driving force toward the aCSF for any released molecules. After
338 4h incubation the amount of the released KYNA was more than 30 times higher than that
339 retained in the tissue **(See Supp. Fig. 2.)**. This release mechanism of KYNA is still unknown
340 and should also be investigated in future work. Nevertheless, a high local KYNA
341 concentration might be reached upon L-KYN treatment in the close apposition of the KYNA
342 release sites.
343 It is important to note that our results regarding KYNA production may not reflect completely
344 the *in vivo* mechanisms. The brain-to-blood elimination of brain KYNA through probenecid-
345 sensitive organic acid transport is continuous *in vivo* (Miller et al., 1992), however, the ratio
346 of elimination in the mice is not described. Furthermore, the composition of aCSF differs in
347 several aspects from the *in vivo* physiological extracellular milieu. For instance, there are no
348 amino acids in the aCSF (e.g. aspartate, tryptophan), which can negatively impact the activity
349 of the KAT isoenzymes (Han et al., 2010b). The applied incubation temperature was lower
350 than physiological, but higher temperature curtails the lifespan of acute slices as a
351 consequence of bacterial growth and cellular metabolism (Buskila et al., 2014). Lower
352 temperature slows down these adverse processes and prolong the time period during which
353 the slices can be kept functional. Beyond tissue viability aspects, and *in vitro*
354 electrophysiological routines we chose 30 °C for incubation basing on the paper of Banerjee
355 et al. (2012), where this temperature was used as an optimal temperature for KAT-2 (Banerjee
356 et al., 2012). These differences may lead to altered KAT activity and to a modified
357 production of KYNA. However, we did not find altered KAT-2 expression level of the
358 samples incubated under SV condition ($F = 0.000$; $p = 0.989$; Partial Eta Squared: 0.000),
359 therefore a quasi normally KYNA production can be suggested **(Supp. Fig. 3).**

360 The ≈6.3fold elevation in aCSF KYNA content by this small amount of tissue after L-KYN
361 addition indicates a high KAT capacity. Previously it has been shown on purified KAT
362 preparation from rat liver that KATs have high capacity and Km value (~1 mM) for L-KYN

363 (Bender and McCreanor, 1985). Indeed, KYNA production in the rat brain was saturable only
364 at high L-KYN (≈1 mM) concentration (Turski et al., 1989), which is concordant with our
365 findings.
366 In conclusion, mouse brain tissue intensively liberates endogenous and *de novo* synthesized
367 KYNA into the extracellular milieu *in vitro*, whereas the retained KYNA in the tissue is
368 negligible.

369 **4.3 Effect of KAT-2 inhibitor PF-04859989 on *de novo* KYNA release**

370 The advent of highly specific KAT-2 inhibitors opened new perspectives in clarifying KP
371 function in rodents (Dounay et al., 2012, Nematollahi et al., 2016). However, no
372 pharmacological experiment has yet targeted the mouse KAT-2 function, probably because of
373 its proposed irrelevance (Guidetti et al., 2007). In our previous anatomical study, we found
374 prominent KAT-2 immunopositivity in astrocytes and in GABAergic cells in the adult mouse
375 brain (Heredi et al., 2017). We therefore hypothesized that KAT-2 has a specific role in
376 mouse brain KYNA function. Because of the low basal KYNA content of the tissue
377 homogenate and that of the aCSF (usually close to the detection limit of HPLC), we estimated
378 the effect of the inhibitor on the KYN induced *de novo* KYNA production.
379 Applying the highly specific KAT-2 inhibitor PF-04859989 in a similar concentration, which
380 was found in the rat CSF after parenteral application (Dounay et al., 2012), resulted in a
381 decrease of *de novo* KYNA production by almost 40%. Although, this is higher than has
382 previously been reported using alternative methods, KYNA production was not completely
383 abolished following KAT-2 inhibition; 60% of total KAT activity remained. This indicates
384 that, in a whole other KAT enzymes make a greater contribution in the mouse brain, however,
385 it does not exclude the important role of mouse KAT-2. Indeed, an incomplete inhibition of
386 KAT activity is more suitable in the experimental models of therapeutical KYNA level
387 reduction. Our results indicate that the investigation of the effects of pharmacological KAT-2
388 inhibition should be extended to mouse models, which was largely neglected in this relation.
389

390 **Acknowledgments**
391 Thanks are due to Matthew Higginson for grammar proofreading.
392

393 **Funding**
394 This study was supported by grant GINOP 2.3.2-15-2016-00034 and co-financed by EFOP-
395 3.6.1-16-2016-00008 grant and grant by MTA-SZTE Neuroscience Research group. LG, JH,

JT, ZsK, LV, EO were fellows in the JSPS-HAS mobility scholarship program (NKM-48/2017). Dénes Zádori was supported by the János Bolyai Scholarship of the Hungarian Academy of Sciences.

Conflict of interest

The authors declare no competing financial interests. All co-author agree with the submission of this form of the manuscript.

5 References

Albuquerque EX, Schwarcz R (2013) Kynurenic acid as an antagonist of alpha7 nicotinic acetylcholine receptors in the brain: facts and challenges. Biochem Pharmacol 85:1027-1032.

Alexander KS, Wu HQ, Schwarcz R, Bruno JP (2012) Acute elevations of brain kynurenic acid impair cognitive flexibility: normalization by the alpha7 positive modulator galantamine. Psychopharmacology (Berl) 220:627-637.

Alkondon M, Pereira EF, Eisenberg HM, Kajii Y, Schwarcz R, Albuquerque EX (2011) Age dependency of inhibition of alpha7 nicotinic receptors and tonically active N-methyl-D-aspartate receptors by endogenously produced kynurenic acid in the brain. J Pharmacol Exp Ther 337:572-582.

Alkondon M, Pereira EF, Todd SW, Randall WR, Lane MV, Albuquerque EX (2015) Functional G-protein-coupled receptor 35 is expressed by neurons in the CA1 field of the hippocampus. Biochem Pharmacol 93:506-518.

Alkondon M, Pereira EF, Yu P, Arruda EZ, Almeida LE, Guidetti P, Fawcett WP, Sapko MT, Randall WR, Schwarcz R, Tagle DA, Albuquerque EX (2004) Targeted deletion of the kynurenine aminotransferase ii gene reveals a critical role of endogenous kynurenic acid in the regulation of synaptic transmission via alpha7 nicotinic receptors in the hippocampus. J Neurosci 24:4635-4648.

Amaral M, Outeiro TF, Scrutton NS, Giorgini F (2013) The causative role and therapeutic potential of the kynurenine pathway in neurodegenerative disease. Journal of molecular medicine 91:705-713.

Artru A.A. (1993) Cerebrospinal Fluid: Physiology and Pharmacology. In: Sperry R.J., Johnson J.O., Stanley T.H. (eds) Anesthesia and the Central Nervous System. Developments in Critical Care Medicine and Anesthesiology, vol 28. Springer, Dordrecht

Banerjee J, Alkondon M, Albuquerque EX (2012a) Kynurenic acid inhibits glutamatergic transmission to CA1 pyramidal neurons via alpha7 nAChR-dependent and -independent mechanisms. Biochem Pharmacol 84:1078-1087.

Banerjee J, Alkondon M, Pereira EF, Albuquerque EX (2012b) Regulation of GABAergic inputs to CA1 pyramidal neurons by nicotinic receptors and kynurenic acid. J Pharmacol Exp Ther 341:500-509.

Bender DA, McCreanor GM (1985) Kynurenine hydroxylase: a potential rate-limiting enzyme in tryptophan metabolism. Biochem Soc Trans 13:441-443.

Berlinguer-Palmini R, Masi A, Narducci R, Cavone L, Maratea D, Cozzi A, Sili M, Moroni F, Mannaioni G (2013) GPR35 activation reduces Ca2+ transients and contributes to the kynurenic acid-dependent reduction of synaptic activity at CA3-CA1 synapses. PLoS One 8:e82180.

Birch PJ, Grossman CJ, Hayes AG (1988) Kynurenic acid antagonises responses to NMDA via an action at the strychnine-insensitive glycine receptor. Eur J Pharmacol 154:85-87.

Buskila Y, Breen PP, Tapson J, van Schaik A, Barton M, Morley JW (2014) Extending the viability of acute brain slices. Scientific reports 4:5309.

Cho S, Wood A, Bowlby MR (2007) Brain slices as models for neurodegenerative disease and screening platforms to identify novel therapeutics. Curr Neuropharmacol 5:19-33.

Chuquet J, Quilichini P, Nimchinsky EA, Buzsaki G (2010) Predominant enhancement of glucose uptake in astrocytes versus neurons during activation of the somatosensory cortex. J Neurosci 30:15298-15303.

Davolio C, Greenamyre JT (1995) Selective vulnerability of the CA1 region of hippocampus to the indirect excitotoxic effects of malonic acid. Neurosci Lett 192:29-32.

Dounay AB, Anderson M, Bechle BM, Campbell BM, Claffey MM, Evdokimov A, Evrard E, Fonseca KR, Gan X, Ghosh S, Hayward MM, Horner W, Kim JY, McAllister LA, Pandit J, Paradis V, Parikh VD, Reese MR, Rong S, Salafia MA, Schuyten K, Strick CA, Tuttle JB, Valentine J, Wang H, Zawadzke LE, Verhoest PR (2012) Discovery of Brain-Penetrant, Irreversible Kynurenine Aminotransferase II Inhibitors for Schizophrenia. ACS medicinal chemistry letters 3:187-192.

457 Dounay AB, Tuttle JB, Verhoest PR (2015) Challenges and Opportunities in the Discovery of New
458 Therapeutics Targeting the Kynurenine Pathway. J Med Chem 58:8762-8782.
459 Fujigaki S, Saito K, Takemura M, Fujii H, Wada H, Noma A, Seishima M (1998) Species differences in L-
460 tryptophan-kynurenine pathway metabolism: quantification of anthranilic acid and its
461 related enzymes. Arch Biochem Biophys 358:329-335.
462 Fukuda A, Czurko A, Hida H, Muramatsu K, Lenard L, Nishino H (1995) Appearance of deteriorated
463 neurons on regionally different time tables in rat brain thin slices maintained in physiological
464 condition. Neurosci Lett 184:13-16.
465 Gal EM, Sherman AD (1980) L-kynurenine: its synthesis and possible regulatory function in brain.
466 Neurochem Res 5:223-239.
467 Guidetti P, Amori L, Sapko MT, Okuno E, Schwarcz R (2007) Mitochondrial aspartate
468 aminotransferase: a third kynurenate-producing enzyme in the mammalian brain. J
469 Neurochem 102:103-111.
470 Han Q, Cai T, Tagle DA, Li J (2010a) Structure, expression, and function of kynurenine
471 aminotransferases in human and rodent brains. Cellular and molecular life sciences : CMLS
472 67:353-368.
473 Han Q, Cai T, Tagle DA, Li J (2010b) Thermal stability, pH dependence and inhibition of four murine
474 kynurenine aminotransferases. BMC Biochem 11:19.
475 Heredi J, Berko AM, Jankovics F, Iwamori T, Iwamori N, Ono E, Horvath S, Kis Z, Toldi J, Vecsei L,
476 Gellert L (2017) Astrocytic and neuronal localization of kynurenine aminotransferase-2 in the
477 adult mouse brain. Brain Struct Funct 222:1663-1672.
478 Hodgkins PS, Wu HQ, Zielke HR, Schwarcz R (1999) 2-Oxoacids regulate kynurenic acid production in
479 the rat brain: studies in vitro and in vivo. J Neurochem 72:643-651.
480 Kovalenko T, Osadchenko I, Nikonenko A, Lushnikova I, Voronin K, Nikonenko I, Muller D, Skibo G
481 (2006) Ischemia-induced modifications in hippocampal CA1 stratum radiatum excitatory
482 synapses. Hippocampus 16:814-825.
483 Lein PJ, Barnhart CD, Pessah IN (2011) Acute hippocampal slice preparation and hippocampal slice
484 cultures. Methods Mol Biol 758:115-134.
485 Lundgaard I, Li B, Xie L, Kang H, Sanggaard S, Haswell JD, Sun W, Goldman S, Blekot S, Nielsen M,
486 Takano T, Deane R, Nedergaard M (2015) Direct neuronal glucose uptake heralds activity-
487 dependent increases in cerebral metabolism. Nature communications 6:6807.
488 Miller JM, MacGarvey U, Beal MF (1992) The effect of peripheral loading with kynurenine and
489 probenecid on extracellular striatal kynurenic acid concentrations. Neurosci Lett 146:115-
490 118.
491 Moroni F, Russi P, Lombardi G, Beni M, Carla V (1988) Presence of kynurenic acid in the mammalian
492 brain. J Neurochem 51:177-180.
493 Nematollahi A, Sun G, Jayawickrama GS, Church WB (2016) Kynurenine Aminotransferase Isozyme
494 Inhibitors: A Review. International journal of molecular sciences 17.
495 Okuno A, Fukuwatari T, Shibata K (2011) High tryptophan diet reduces extracellular dopamine
496 release via kynurenic acid production in rat striatum. J Neurochem 118:796-805.
497 Olsson SK, Larsson MK, Erhardt S (2012) Subchronic elevation of brain kynurenic acid augments
498 amphetamine-induced locomotor response in mice. J Neural Transm (Vienna) 119:155-163.
499 Potter MC, Elmer GI, Bergeron R, Albuquerque EX, Guidetti P, Wu HQ, Schwarcz R (2010) Reduction
500 of endogenous kynurenic acid formation enhances extracellular glutamate, hippocampal
501 plasticity, and cognitive behavior. Neuropsychopharmacology 35:1734-1742.
502 Prescott C, Weeks AM, Staley KJ, Partin KM (2006) Kynurenic acid has a dual action on AMPA
503 receptor responses. Neurosci Lett 402:108-112.
504 Rosenthal N, Brown S (2007) The mouse ascending: perspectives for human-disease models. Nature
505 cell biology 9:993-999.
506 Scharfman HE, Hodgkins PS, Lee SC, Schwarcz R (1999) Quantitative differences in the effects of de
507 novo produced and exogenous kynurenic acid in rat brain slices. Neurosci Lett 274:111-114.

Schwieler L, Erhardt S, Nilsson L, Linderholm K, Engberg G (2006) Effects of COX-1 and COX-2 inhibitors on the firing of rat midbrain dopaminergic neurons--possible involvement of endogenous kynurenic acid. Synapse 59:290-298.

Swartz KJ, During MJ, Freese A, Beal MF (1990) Cerebral synthesis and release of kynurenic acid: an endogenous antagonist of excitatory amino acid receptors. J Neurosci 10:2965-2973.

Turski WA, Gramsbergen JB, Traitler H, Schwarcz R (1989) Rat brain slices produce and liberate kynurenic acid upon exposure to L-kynurenine. J Neurochem 52:1629-1636.

Urbanska EM, Chmielewski M, Kocki T, Turski WA (2000) Formation of endogenous glutamatergic receptors antagonist kynurenic acid--differences between cortical and spinal cord slices. Brain Res 878:210-212.

Vecsei L, Szalardy L, Fulop F, Toldi J (2013) Kynurenines in the CNS: recent advances and new questions. Nature reviews Drug discovery 12:64-82.

Zmarowski A, Wu HQ, Brooks JM, Potter MC, Pellicciari R, Schwarcz R, Bruno JP (2009) Astrocyte-derived kynurenic acid modulates basal and evoked cortical acetylcholine release. Eur J Neurosci 29:529-538.

525 ## Legend to figures

526 **Fig. 1: Glucose consumption in the course of 4h SV incubation.** Acute slices were
527 incubated as routinely in aCSF having high glucose concentration (10mM). Glucose
528 concentration was already dropped after 30 min (≈8%), however, the decrease was not
529 statistically significant (F=4,281; p=0,072; Partial Eta Squared: 0,349). 4h incubation,
530 however, resulted in a significant decrease of aCSF glucose content (≈20%) (F=20,304;
531 p=0,002; Partial Eta Squared: 0,717). Data are expressed as a percentage of baseline glucose
532 content (glucose content of the aCSF at the starting point of the experiment) and represent the
533 mean ± SD. n=5 animals, 6+6 corresponding brain slices per condition.
534

535 **Fig. 2: LDH release in the course of 4h SV incubation.** At the beginning of the incubation
536 aCSF LDH content is virtually zero (only measuring error is depicted). In comparison,
537 gradual increase of the aCSF LDH content could be measured in the course of 30 min (Z=
538 16,910; p= 0,959) and 4h incubation (Z= 16,910; p=0,030). However Triton X-100 treatment
539 resulted in a ≈14 fold increase of LDH in the aCSF after 4h (Z= 16,910; p=0,001). This
540 indicates that the cell membrane integrity is largely preserved in the case of 4h incubation.
541 Data represent the mean ± SD. n=9 animals, 6+6 corresponding brain slices per condition.
542

543 **Fig. 3: Cresyl violet staining (A-B) and NeuN immunolabelling (C-D) in the dorsal**
544 **hippocampus of mouse acute brain slices.** There was no visible difference between the LV
545 **(A-C)** and SV **(B-D)** group in the CA1 area of the hippocampus after 4h incubation. Cells
546 keep their normal appearing in the pyramidal cell layer. Scale bars are 100 µm.

547 **Fig. 4: Basal glutamatergic synaptic properties of acute brain slices.** There is no
548 significant difference between slices recorded immediately after post-slicing recovery period
549 (30 min.), or incubated under LV condition for 4hours and under SV conditions, respectively
550 (F=0.793; p=0,465; Partial Eta Squared: 0,064). The values represent normalized means±SD
551 and were plotted as a function of stimulus strength. n=17 animals; 11+9+8 recordings/group.

552 **Fig. 5: Basal and *de novo* KYNA content in the incubating aCSF and in the tissue**
553 **homogenate after 4h incubation.** Without L-KYN administration 7.01±2.03ng basal KYNA
554 content could be measured from the aCSF and 0.22±0.07ng from the brain tissue homogenate.
555 In contrast, as a result of 10 µM L-KYN administration we found a 6.3 fold increase in the
556 aCSF (44.56 ±6,99ng) (Z=6,818; p= 0,009) and a 3.8 fold increase in the tissue (0.85±0.21ng)
557 KYNA content. The values represent means ±SD. n=5 animals, 6+6 corresponding brain
558 slices per condition.

559 **Fig. 6: Effect of KAT-2 inhibitor PF-04859989 on de novo KYNA release.** Acute slices
560 were incubated in the presence of 10µM L-KYN with or without PF-04859989 in a
561 concentration of 5µM. KYNA content of the aCSF was measured after 4h incubation. High
562 KYNA content could be measured in the L-KYN group (55.19±6.45ng). Addition of the
563 inhibitor resulted in a significant decrease of the released KYNA in the aCSF by almost 40%
564 (34.5±6.93ng; F=23,868; p=0,001; Partial Eta Squared: 0,749). The values represent
565 means±SD. n=5 animals, 6+6 corresponding brain slices per condition.

566

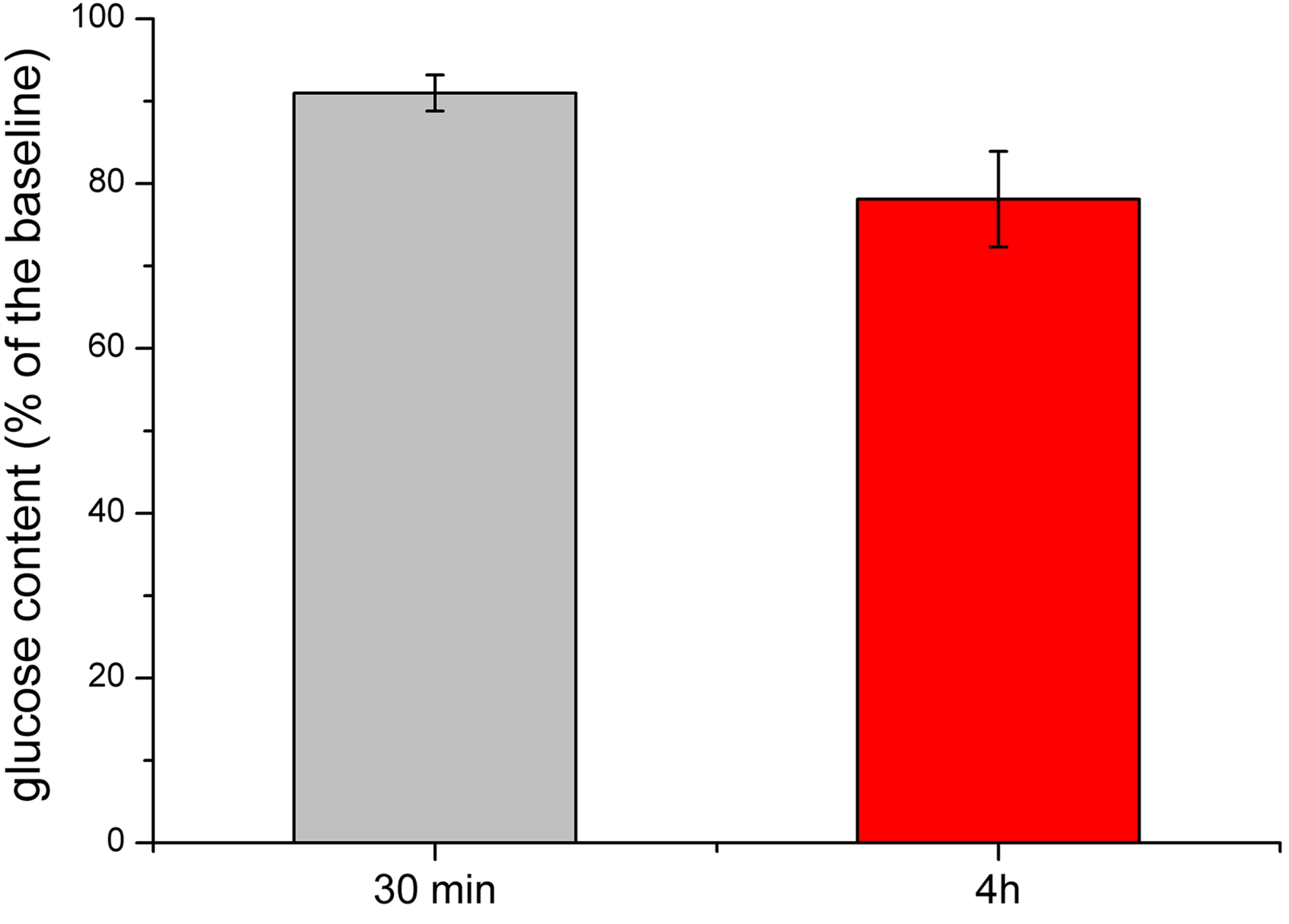
glucose content (% of the baseline)
100
80
60
40
20
0
30 min
4h

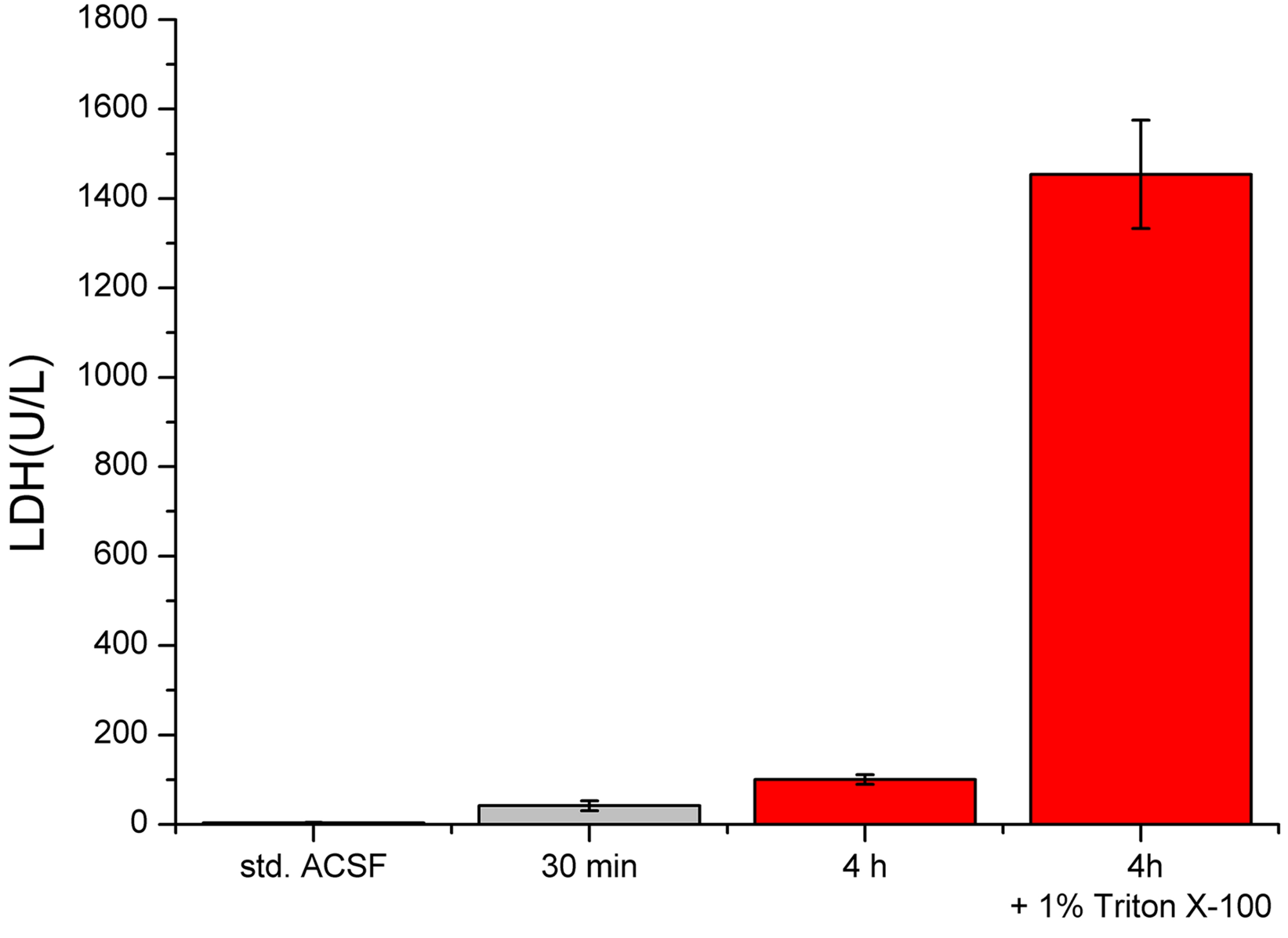
LDH(U/L)
1800
1600
1400
1200
1000
800
600
400
200
0
std. ACSF
30 min
4 h
4h
+ 1% Triton X-100

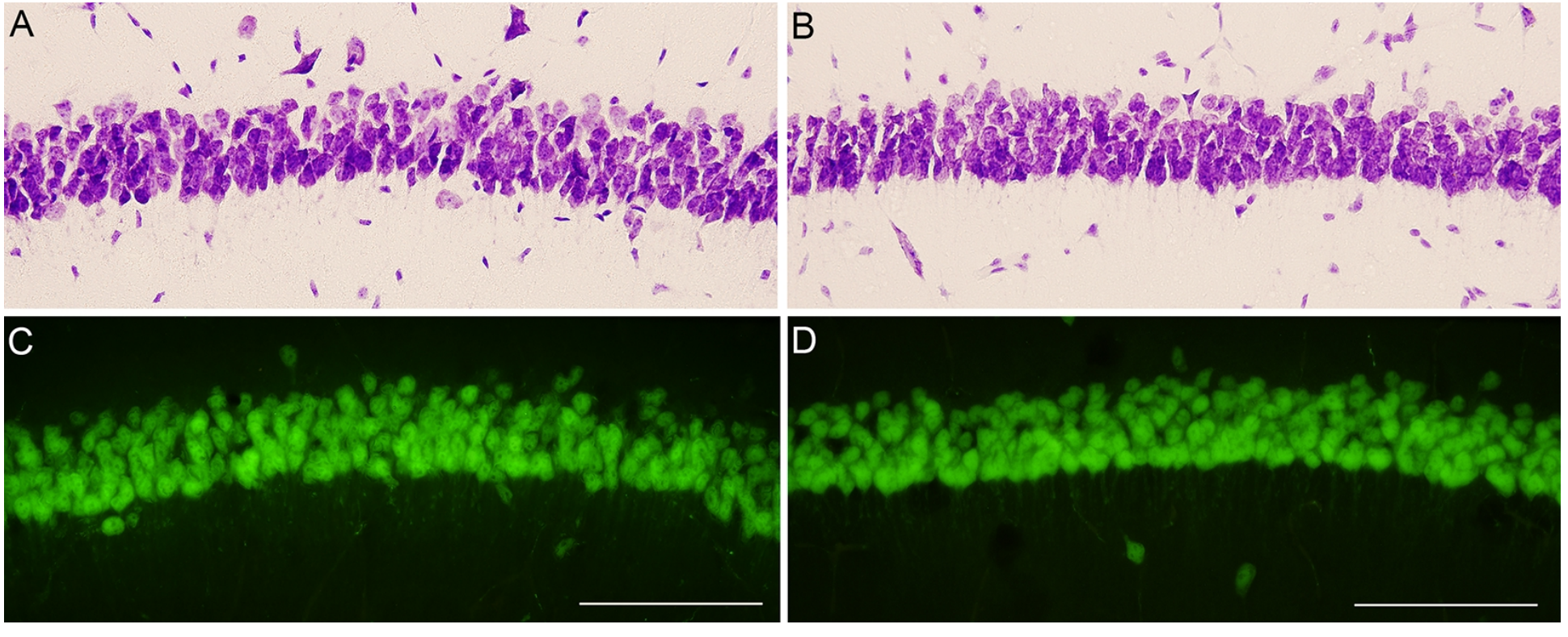
A
B
C
D

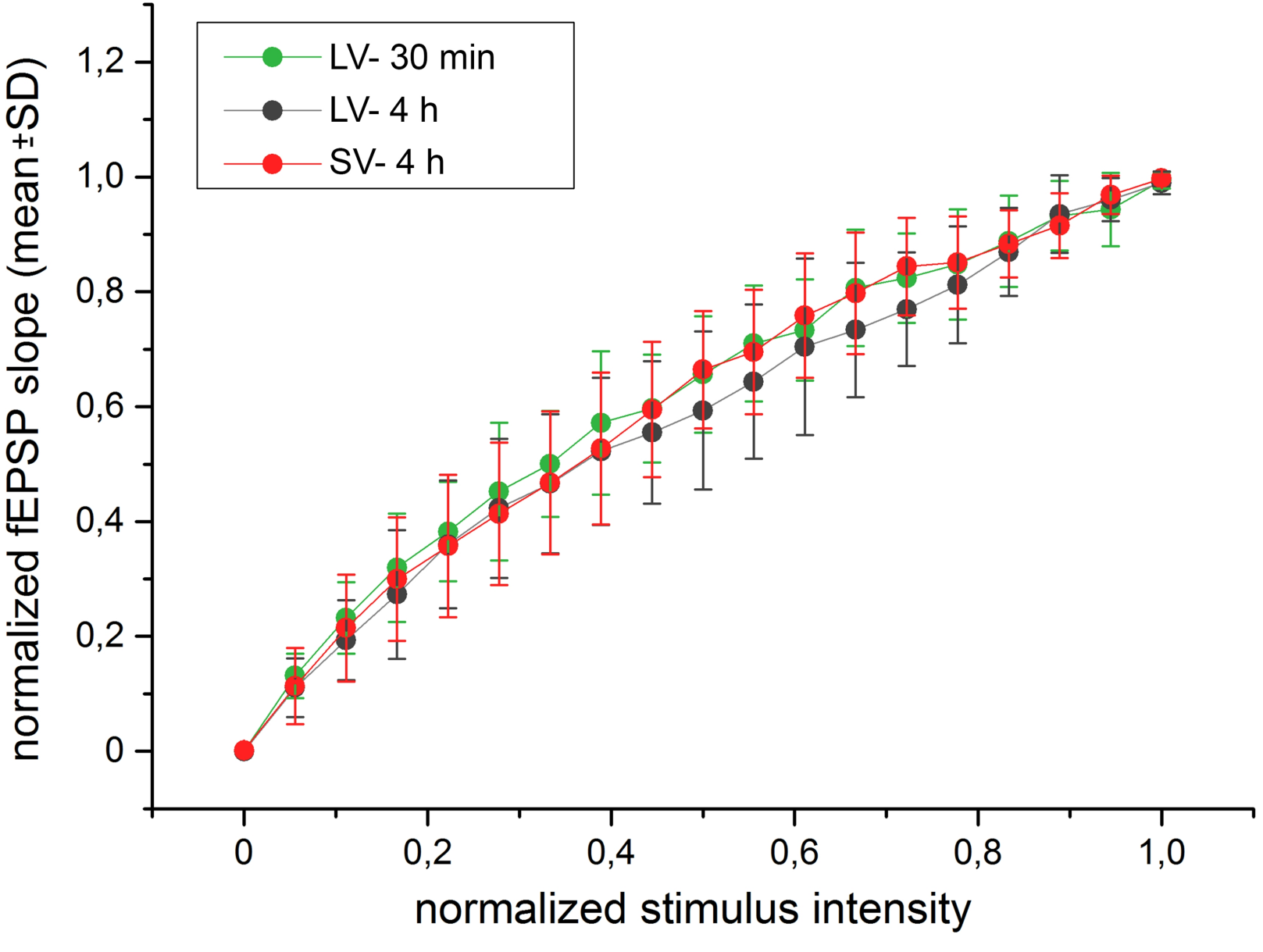
LV- 30 min
LV- 4 h
SV- 4 h
normalized fEPSP slope (mean±SD)
1,2
1,0
0,8
0,6
0,4
0,2
0
0
0,2
0,4
0,6
0,8
1,0
normalized stimulus intensity

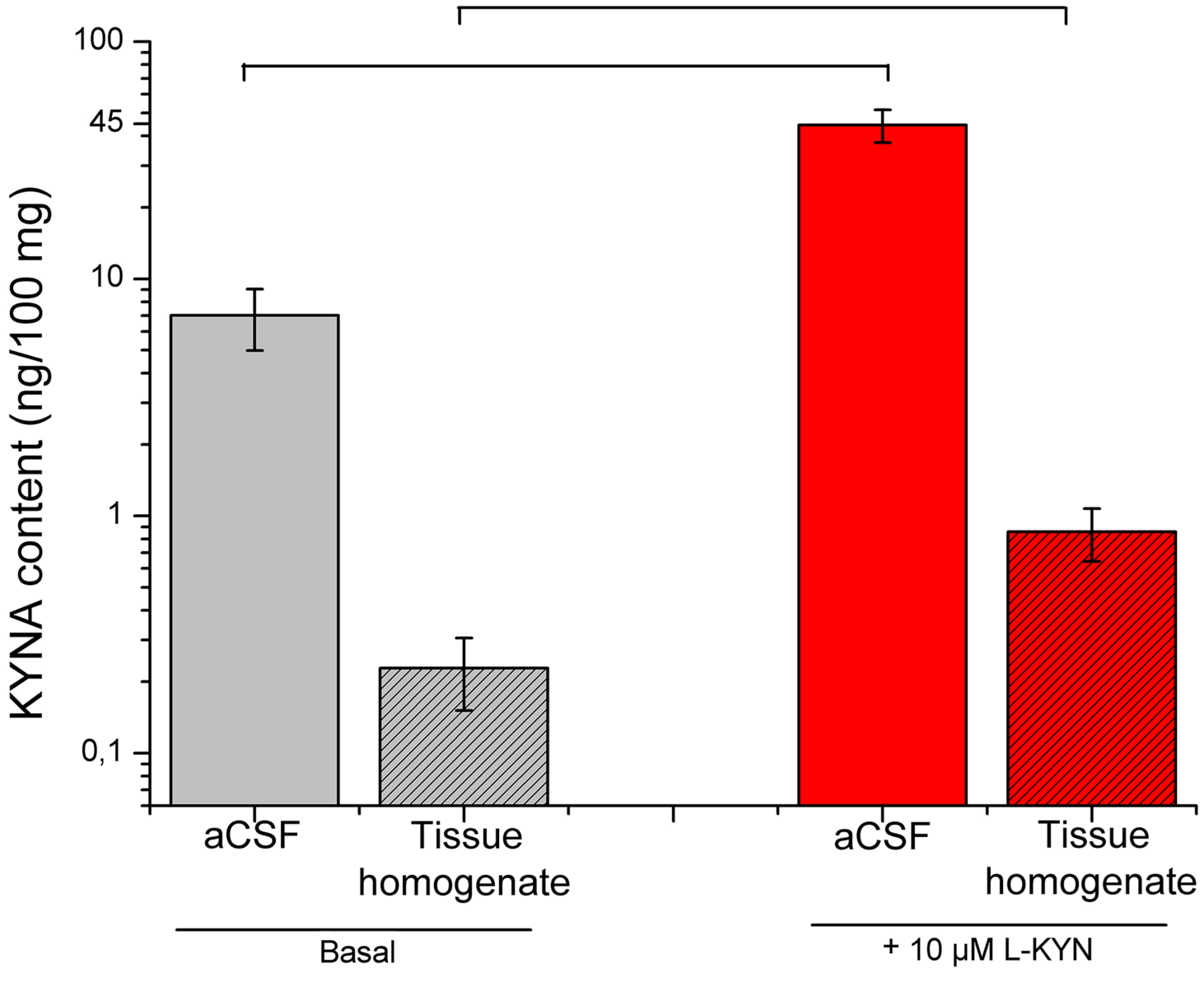
KYNA content (ng/100 mg)
100
45
10
1
0,1
aCSF
Tissue homogenate
aCSF
Tissue homogenate
Basal
+ 10 µM L-KYN

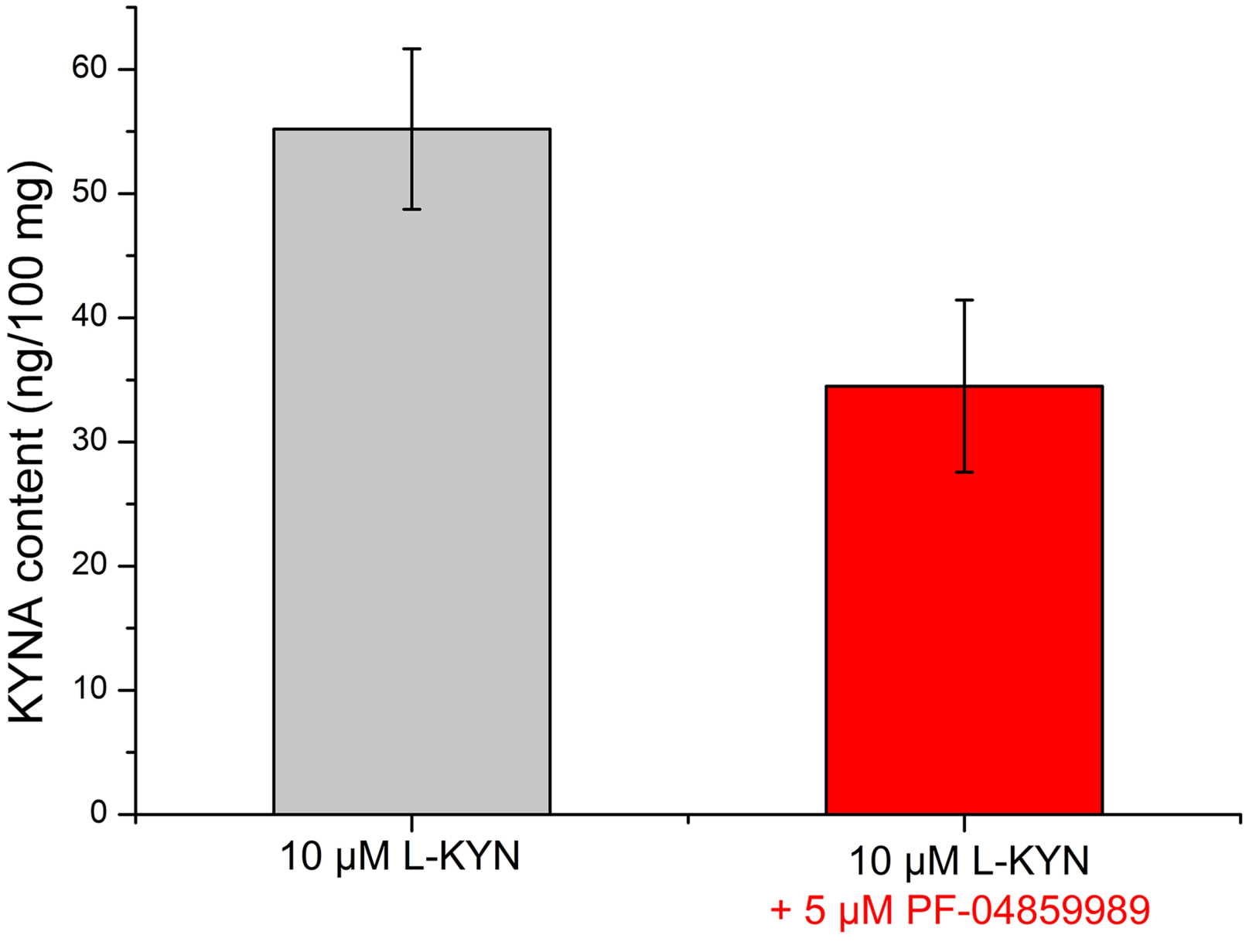
KYNA content (ng/100 mg)
0
10
20
30
40
50
60
10 μM L-KYN
10 μM L-KYN
+ 5 μM PF-04859989

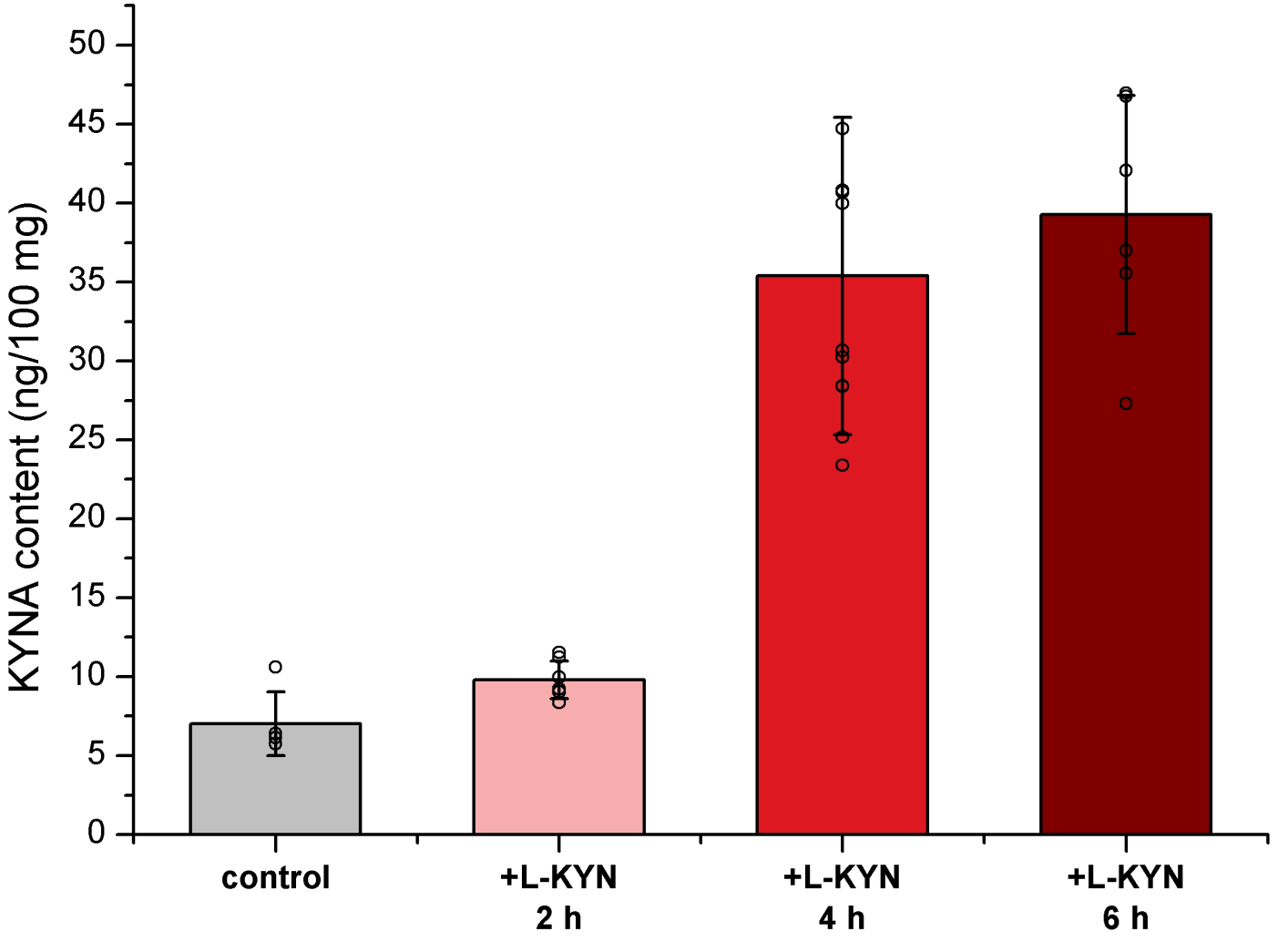
KYNA content (ng/100 mg)
0
5
10
15
20
25
30
35
40
45
50
control
+L-KYN
2 h
+L-KYN
4 h
+L-KYN
6 h

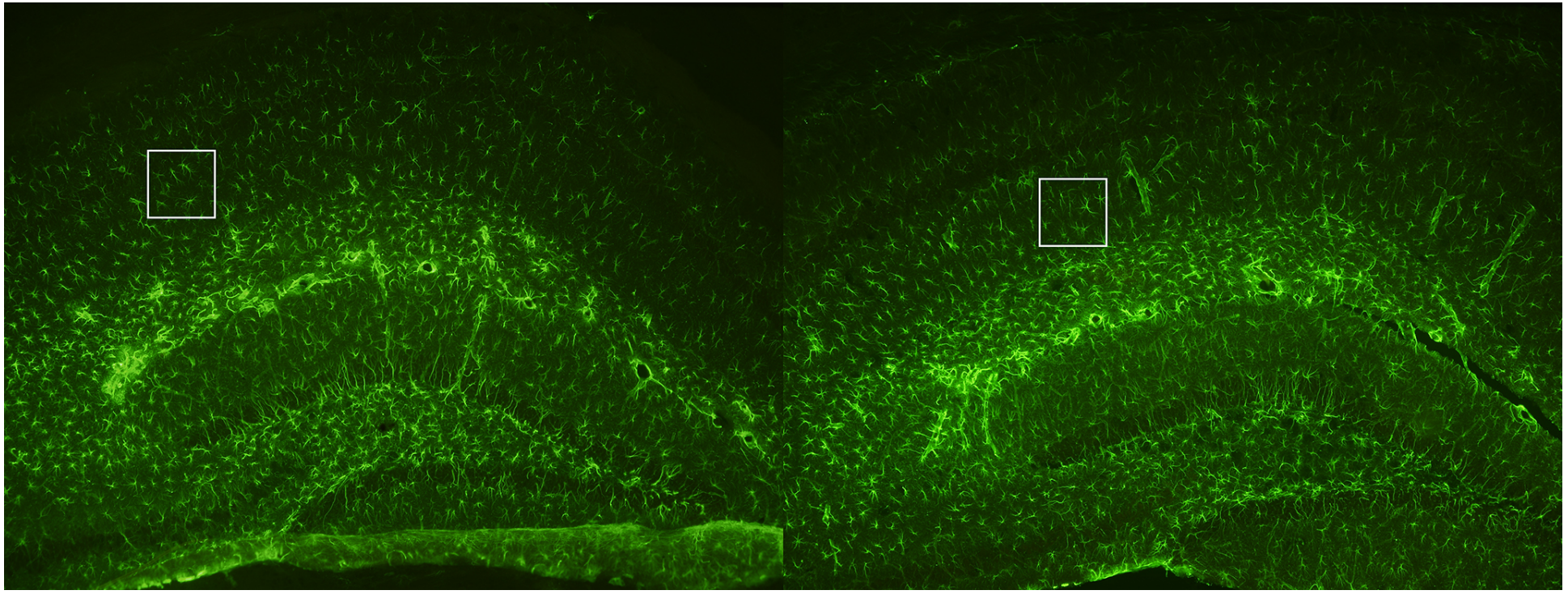

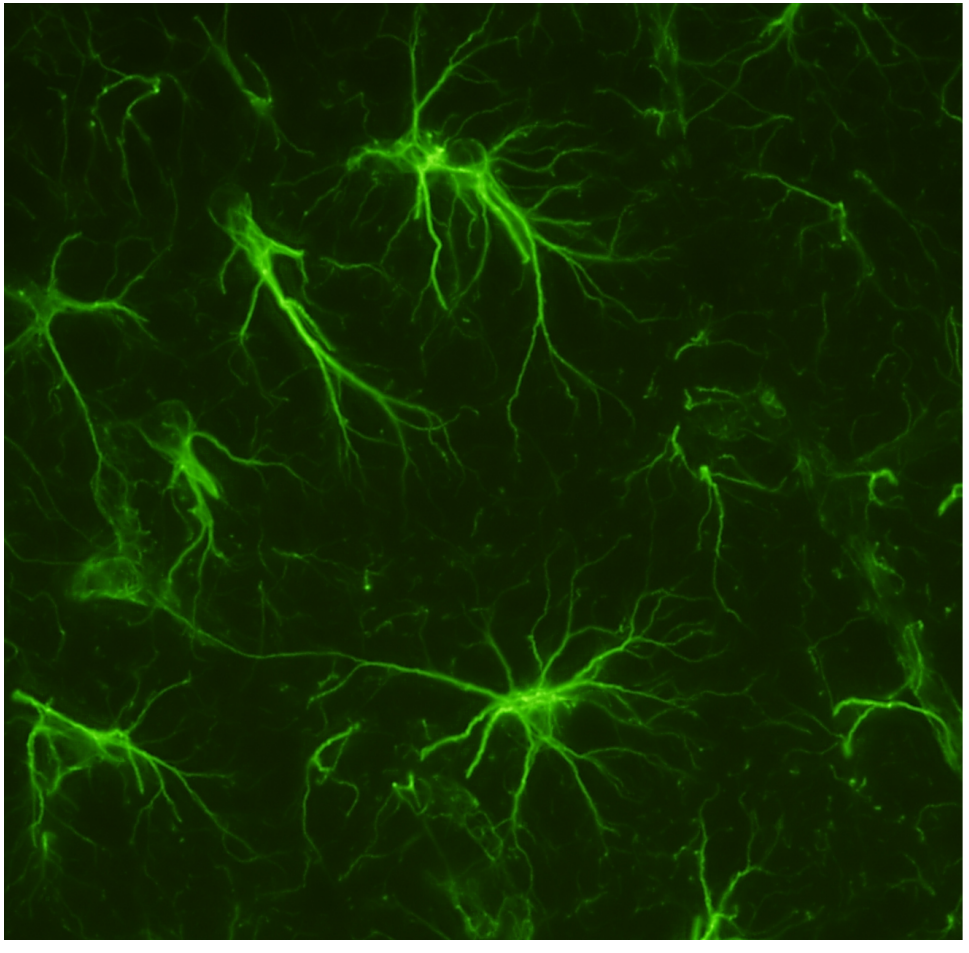

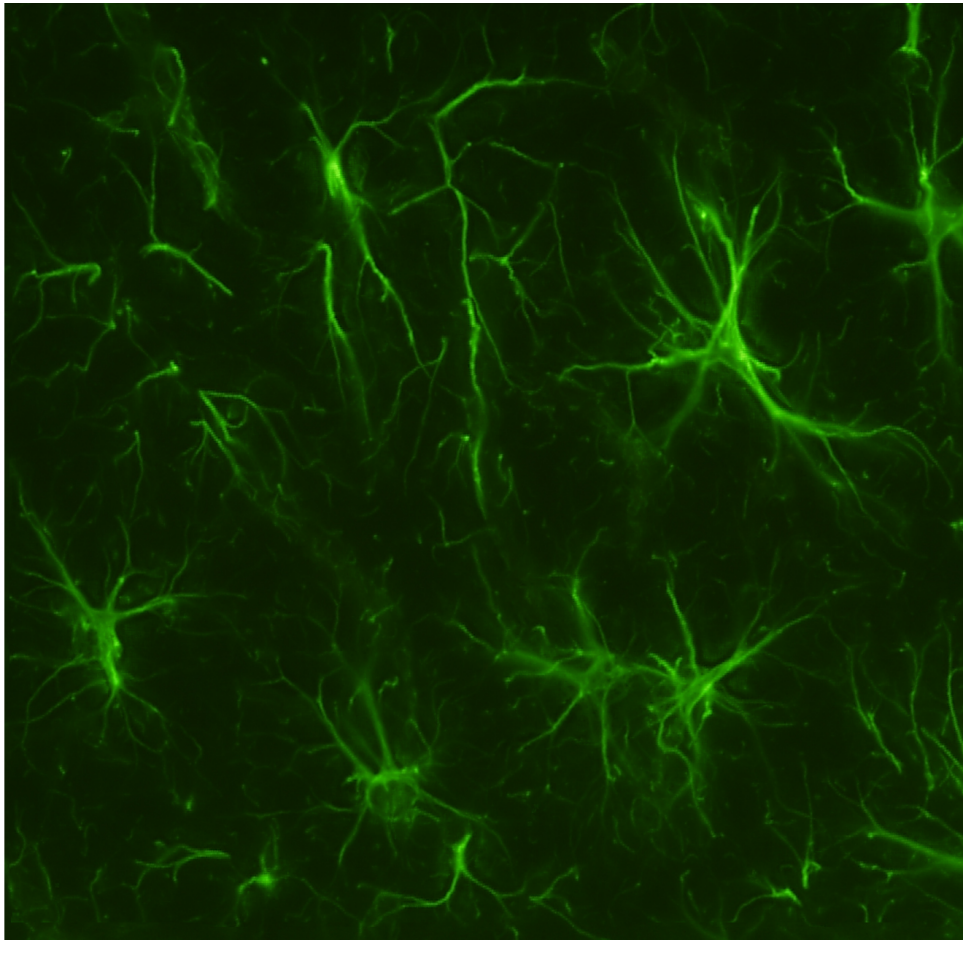

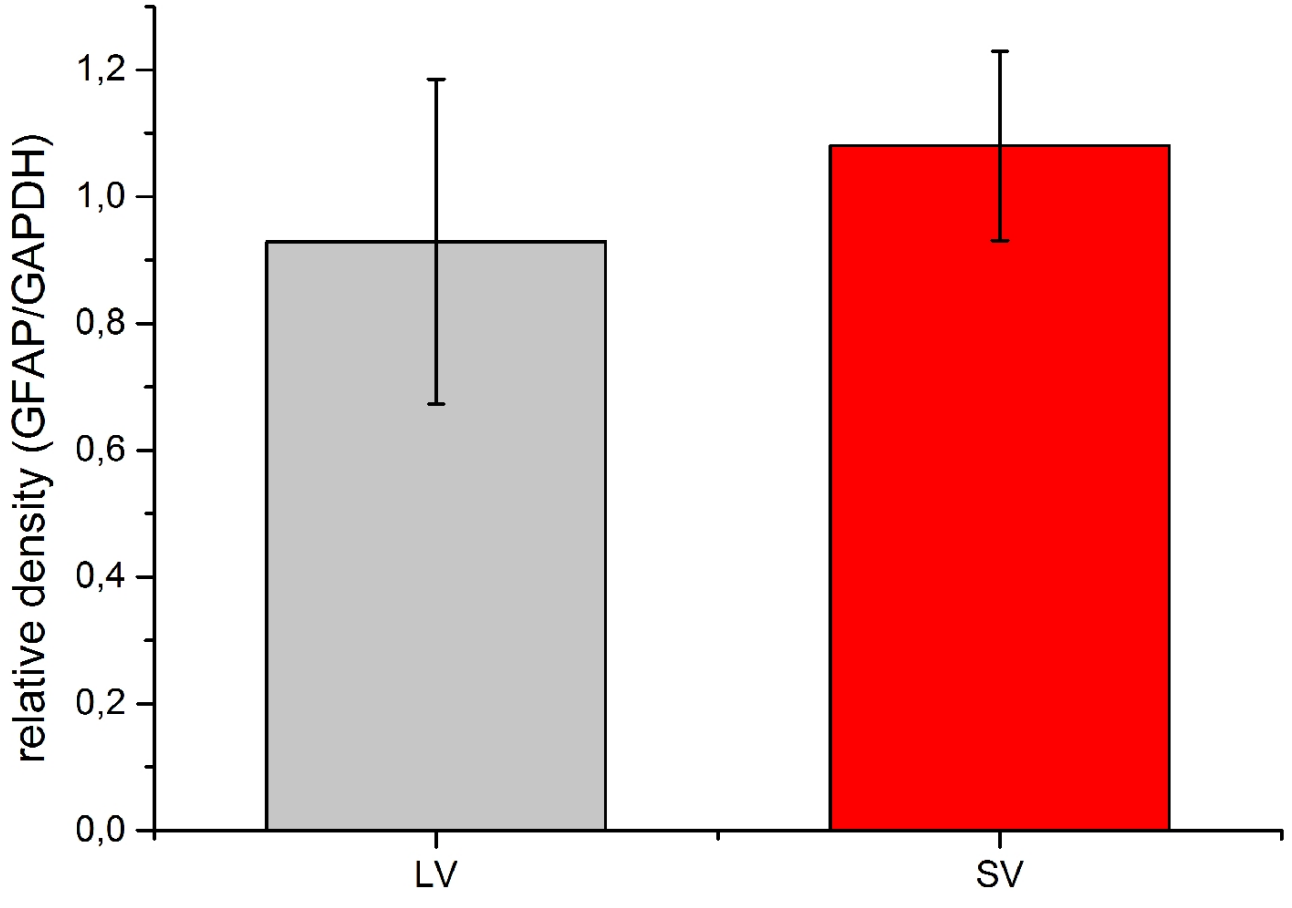
relative density (GFAP/GAPDH)
1,2
1,0
0,8
0,6
0,4
0,2
0,0
LV
SV

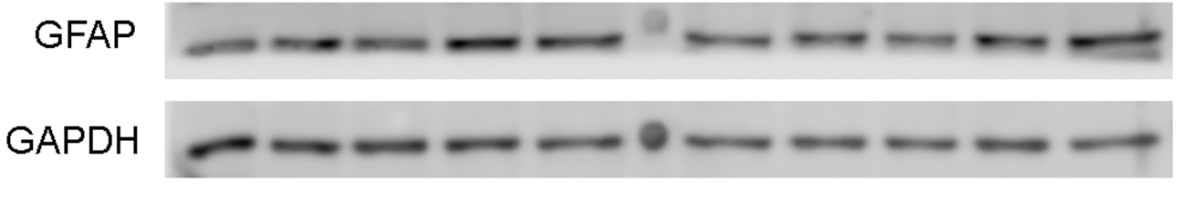
GFAP
GAPDH

Investigating KYNA production and kynurenergic manipulation on acute mouse brain slice preparations

Judit Herédi[1], Edina Katalin Cseh[2], Anikó Magyariné Berkó[1], Gábor Veres[2], Dénes Zádori[2], József Toldi[1], Zsolt Kis[1],László Vécsei[2,3],Etsuro Ono[4];Levente Gellért[1,5,*]

[1]Department of Physiology, Anatomy and Neuroscience, Faculty of Science and Informatics, University of Szeged, Közép Fasor 52., Szeged 6726, Hungary.

[2]Department of Neurology, Faculty of Medicine, University of Szeged, Semmelweis st.6, Szeged 6725 Hungary

[3]MTA-SZTE Neuroscience Research Group, University of Szeged, Semmelweis st. 6, Szeged 6725, Hungary.

[4]Department of Biomedicine, Graduate School of Medical Sciences, Kyushu University Fukuoka, Japan; Center of Biomedical Research, Research Center for Human Disease Modeling, Graduate School of Medical Sciences, Kyushu University Fukuoka, Japan.

[5]Institute of Physiology, University Medical Center of the Johannes Gutenberg University Mainz, Duesbergweg 6, D-55128 Mainz, Germany.

We herewith make a clear statement that the work has not been published elsewhere, and it is not under review with another journal. All co-author agree with the submission of this form of the manuscript. The authors declare no competing financial interests.

AUTHOR DECLARATION

We wish to confirm that there are no known conflicts of interest associated with this publication and there has been no significant financial support for this work that could have influenced its outcome.

We confirm that the manuscript has been read and approved by all named authors and that there are no other persons who satisfied the criteria for authorship but are not listed. We further confirm that the order of authors listed in the manuscript has been approved by all of us.

We confirm that we have given due consideration to the protection of intellectual property associated with this work and that there are no impediments to publication, including the timing of publication, with respect to intellectual property. In so doing we confirm that we have followed the regulations of our institutions concerning intellectual property.

We further confirm that any aspect of the work covered in this manuscript that has involved experimental animals has been conducted with the ethical approval of all relevant bodies and that such approvals are acknowledged within the manuscript.

We understand that the Corresponding Author is the sole contact for the Editorial process (including Editorial Manager and direct communications with the office). He/she is responsible for communicating with the other authors about progress, submissions of revisions and final approval of proofs. We confirm that we have provided a current, correct email address which is accessible by the Corresponding Author and which has been configured to accept email from gellert.levente1@gmail.com

Signed by all authors as follows:

Judit Herédi[1]	21.11.2018 date
Levente Gellért[1,2]	21.11.2018 date
Anikó Magyariné Berkó [1]	21.11.2018. date
Zsolt Kis[1]	21.11.2018. date
József Toldi[1]	21.11.2018. date

[1]Department of Physiology, Anatomy and Neuroscience, Faculty of Science and Informatics, University of Szeged, Közép Fasor 52., Szeged 6726, Hungary

[2]Institute of Physiology, University Medical Center of the Johannes Gutenberg University Mainz, Duesbergweg 6, D-55128 Mainz, Germany

..... 22/11/2018
Dénes Zádori[3] date

..... 22/11/2018
Gábor Veres[3] date

..... 22/11/2018
László Vécsei[3, 4] date

..... 22/11/2018
Edina Katalin Cseh[3] date

[3]Department of Neurology, Faculty of Medicine, University of Szeged, Semmelweis st.6, Szeged 6725, Hungary

[4]MTA-SZTE Neuroscience Research Group, University of Szeged, Semmelweis st. 6, Szeged 6725, Hungary

AUTHOR DECLARATION

We wish to confirm that there are no known conflicts of interest associated with this publication and there has been no significant financial support for this work that could have influenced its outcome.

We confirm that the manuscript has been read and approved by all named authors and that there are no other persons who satisfied the criteria for authorship but are not listed. We further confirm that the order of authors listed in the manuscript has been approved by all of us.

We confirm that we have given due consideration to the protection of intellectual property associated with this work and that there are no impediments to publication, including the timing of publication, with respect to intellectual property. In so doing we confirm that we have followed the regulations of our institutions concerning intellectual property.

We further confirm that any aspect of the work covered in this manuscript that has involved experimental animals has been conducted with the ethical approval of all relevant bodies and that such approvals are acknowledged within the manuscript.

We understand that the Corresponding Author is the sole contact for the Editorial process (including Editorial Manager and direct communications with the office). He/she is responsible for communicating with the other authors about progress, submissions of revisions and final approval of proofs. We confirm that we have provided a current, correct email address which is accessible by the Corresponding Author and which has been configured to accept email from gellert.levente1@gmail.com

Signed by all authors as follows:

Etsuro Ono, DVM, Ph.D.
Professor
Department of Biomedicine
Graduate School of Medical Sciences
Kyushu University
Fukuoka 812-8582
Japan

Date 25th November, 2018

Supplement

Materials and Methods

SDS gel electrophoresis (SDS-PAGE) and Western blot: The protein level of KAT-2 was evaluated with SDS-PAGE and Western blot analysis. Protein from brain slices incubated either in SV or LV condition was extracted in tissue protein extraction buffer containing a protease inhibitor cocktail (T-PER®, Thermo Scientific) using mechanical homogenization (Benchmark Scientific, D1000) and sonication (Clifton). Homogenates were centrifuged for 10 min at 10000 g at 4°C (Heraeus Megafuge 16R, Thermo Scientific). Total protein levels in each sample were quantified by the Bradford assay (Sigma-Aldrich) and 50 µg total protein per lane was loaded onto an 8% (Bio-Rad). Homogenate were separated at 100V for 90 min. Proteins were blotted to a PVDF membrane (Millipore Immobilon®- P) using a transfer buffer containing 20% methanol, 25 mM Tris base and 192 mM glycine at 20V for 90 min.

After blotting, the membrane was washed in 1x PBS containing 0.05% Tween-20 (PBST) and blocked with 5% nonfat dried milk (Bio-Rad). Membranes were probed to the primary antibody (rabbit anti-KAT-2, 1:200) at 4˚C overnight. Next day the membranes were washed extensively and incubated with the HRP-conjugated secondary antibody (HRP-conjugated goat anti-rabbit, 1:20000, Jackson ImmunoResearch) for 1 h at RT. Primary and secondary antibody were diluted in 1X PBST containing 5% nonfat dried milk. The immunoreactive bands were visualized with a chemiluminescent kit (Immobilon Western, Millipore) and digital images were captured with Li-Cor C-DIGIT Blot Scanner. Images were analysed with Image Studio™ Lite.

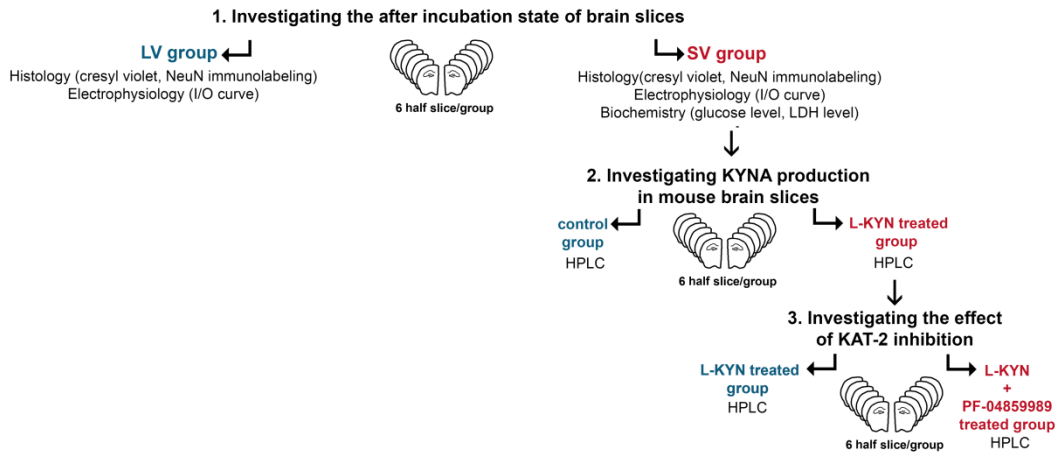

Supp. Fig. 1: Scheme of the experimental protocol. We cut 6 coronal brain slices from the point Bregma -0,9 to -3 and halved every coronal slice for the SV and LV conditions to compare tissue quality (point 1.). The same protocol was used in the case of studying KYNA production (point 2.) and kynurenergic manipulation (point 3.) in the SV condition.

Results

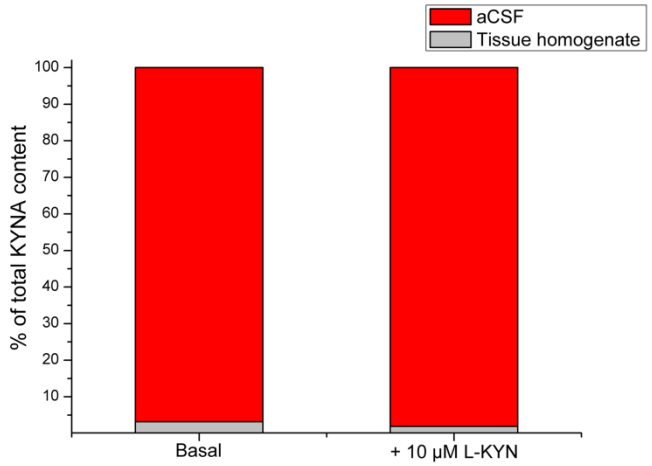

Supp. Fig. 2: Distribution of basal and *de novo* synthesized KYNA after 4 h incubation. ≈97% of the total KYNA content was released to the extracellular compartment (aCSF, red), while only about ≈3% remained in the tissue (grey) under both conditions. Data are expressed as a percentage of total KYNA content.

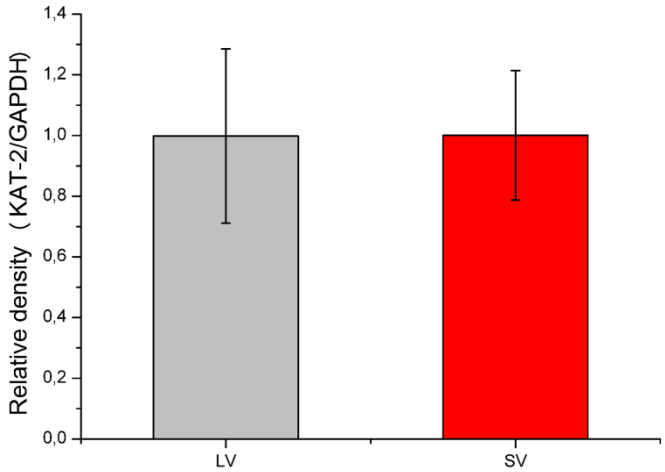

Supp. Fig. 3: KAT-2 protein level of mouse brain slices in the LV (grey) and SV (red) conditions after 4 h incubation. There was no significant difference in KAT-2 protein level between the two groups (F=0,000; p=0,989; Partial Eta Squared:0,000). The values represent means ±SD. n=5animals, 6+6 corresponding brain slices per condition.